# Chronic hypoxia compromises repair of DNA double-strand breaks to drive genetic instability

**Ramya Kumareswaran[1,2], Olga Ludkovski[1], Alice Meng[1], Jenna Sykes[1], Melania Pintilie[1] and Robert G. Bristow[1,2,*]**

[1]Ontario Cancer Institute, Princess Margaret Hospital (University Health Network)
[2]Departments of Medical Biophysics and Radiation Oncology, University of Toronto, Toronto, Ontario, Canada M5G 2M9
*Author for correspondence (rob.bristow@rmp.uhn.on.ca)

*Accepted 22 August 2011*
*Journal of Cell Science 125, 189–199*

*doi: 10.1242/jcs.092262*

## Summary

Hypoxic cells have been linked to genetic instability and tumor progression. However, little is known about the exact relationship between DNA repair and genetic instability in hypoxic cells. We therefore tested whether the sensing and repair of DNA double-strand breaks (DNA-dsbs) is altered in irradiated cells kept under continual oxic, hypoxic or anoxic conditions. Synchronized G0–G1 human fibroblasts were irradiated (0–10 Gy) after initial gassing with 0% $O_2$ (anoxia), 0.2% $O_2$ (hypoxia) or 21% $O_2$ (oxia) for 16 hours. The response of phosphorylated histone H2AX (γ-H2AX), phosphorylated ataxia telangiectasia mutated [ATM(Ser1981)], and the p53 binding protein 1 (53BP1) was quantified by intranuclear DNA repair foci and western blotting. At 24 hours following DNA damage, residual γ-H2AX, ATM(Ser1981) and 53BP1 foci were observed in hypoxic cells. This increase in residual DNA-dsbs under hypoxic conditions was confirmed using neutral comet assays. Clonogenic survival was also reduced in chronically hypoxic cells, which is consistent with the observation of elevated G1-associated residual DNA-dsbs. We also observed an increase in the frequency of chromosomal aberrations in chronically hypoxic cells. We conclude that DNA repair under continued hypoxia leads to decreased repair of G1-associated DNA-dsbs, resulting in increased chromosomal instability. Our findings suggest that aberrant DNA-dsb repair under hypoxia is a potential factor in hypoxia-mediated genetic instability.

**Key words:** DNA double-strand breaks, hypoxia, non-homologous end joining, DNA double-strand break sensors, γ-H2AX, genetic instability

## Introduction

Human cells have evolved specific pathways to repair DNA double-strand breaks (DNA-dsbs) and enact cell cycle checkpoints following DNA damage to ensure genetic stability. These pathways could be oxygen sensitive because endogenous and exogenous DNA damage can be differentially processed and repaired in oxic versus hypoxic cells (Bindra et al., 2007; Bristow and Hill, 2008). For example, intratumoral hypoxia can drive genetic instability and accelerate tumor progression. It can also lead to altered radio- or chemoresistance, enhanced mutagenesis, impaired DNA repair and increased systemic metastasis (reviewed by Bindra et al., 2007; Bristow and Hill, 2008; Huang et al., 2007). The consequence of hypoxic exposure on DNA damage response (DDR) sensing and signalling might relate, in part, to the oxygen level (e.g. hypoxia or anoxia) and the duration of the hypoxic exposure (acute or cycling hypoxia versus chronic or prolonged hypoxia).

One of the most lethal DNA lesions is a DNA-dsb. Incorrectly or non-repaired DNA-dsbs could result in chromosomal deletions, amplifications, aneuploidy and genetic instability (Helleday et al., 2007). Despite the fact that the vast majority of human tumors contain hypoxic sub-regions, little is known about the potential effects of continual hypoxia on DNA-dsb sensing and processing. The signal transduction processes in response to DNA-dsbs are dependent on the kinase activity and autophosphorylation of phosphatidylinositol-3-kinase-related kinases (PIKKs) – ataxia telangiectasia mutated (ATM) and DNA protein kinase (DNA-PKcs) (O'Driscoll and Jeggo, 2006). Current evidence suggests that the MRE11–RAD50–NBS1 (MRN) complex is an initial DNA-dsb sensor that recruits ATM(Ser1981) to the damaged site, and that both ATM and DNA-PKcs are involved in the phosphorylation of the histone H2AX (known as γ-H2AX) (Falck et al., 2005; Rogakou et al., 1998; Stiff et al., 2004). Both microscopy based and co-immunoprecipitation studies have shown that γ-H2AX is required to retain mediator proteins, such as p53 binding protein 1 (53BP1), mediator of DNA damage checkpoint 1 (MDC1), breast cancer 1, early onset (BRCA1), ATM(Ser1981) and the MRN complex at the site of DNA-dsbs until the breaks are repaired (Celeste et al., 2003; Paull et al., 2000). Anoxia has also been shown to activate the ATM and ATR (ataxia telangiectasia and Rad3-related) kinases, resulting in S and G2 cell cycle checkpoint arrests (Freiberg et al., 2006; Gibson et al., 2005; Hammond et al., 2003). However, this activation is in the absence of DNA damage and might be dependent on the oxygen level (Bencokova et al., 2009; Chan et al., 2008).

Subsequent to their detection, DNA-dsbs are primarily repaired by non-homologous end joining (NHEJ), which predominates in the G1 phase, or homologous recombination (HR), which is active during the S and G2 phases. Hypoxia decreases the RNA expression of HR-related genes (*RAD51*, *RAD52*, *RAD54*, *BRCA1*, *BRCA2*) and genes encoding other NHEJ-related proteins (Ku70, DNA-PKcs, DNA ligase IV, Xrcc4) at the mRNA level in asynchronous normal and

malignant cell lines (Meng et al., 2005). However, only the HR-related genes were downregulated at the protein level (Bindra et al., 2005; Bindra et al., 2004; Meng et al., 2005). Decreased RAD51 levels were found to be independent of cell-cycle distribution and the expression of HIF-1α. Hypoxia-mediated decreased expression of the BRCA1 and RAD51 proteins was also associated with decreased HR repair, measured directly by chromosomally based DNA-dsb repair assays (Bindra et al., 2005). These HR-defective cells were more sensitive to DNA-crosslinking agents, providing functional data for hypoxia-mediated HR deficiencies in tumor cells (Chan et al., 2008). Taken together, these data suggest that a functional decrease in the repair of DNA-dsbs under hypoxia might lead to the observed genetic instability and mutator phenotype within the hypoxic microenvironment.

By contrast, functional studies of the repair of DNA-dsbs by NHEJ in the G1 phase of cell cycle under continued hypoxia have not been reported. Previous studies investigated the repair of DNA-dsbs following irradiation of acutely hypoxic cells, which were reoxygenated during repair (Banath et al., 2005; Hammond et al., 2003; Olive and Banath, 2004). Their results were consistent with the oxygen enhancement ratio for initial DNA-dsbs and hypoxic cell radiosensitivity (Bristow and Hill, 2008). Banath and colleagues reported no significant difference in mutation frequency and DNA-dsb repair in oxic and hypoxic subpopulations of V79 Chinese hamster xenografts as measured by Comet assays and γ-H2AX flow cytometry (Banath et al., 2005). However, these experiments addressed DNA-dsb repair under conditions of hypoxia followed by reoxygenation.

At present, very little is known about DNA-dsb repair when non-cycling cells are irradiated and kept under continued hypoxia as a model for cells found in areas of chronic hypoxia within a solid tumor. Such studies might have important implications for the DDR and DNA repair in cancer cells during initial carcinogenesis and angiogenesis and in tumor progression. We hypothesized that similar to our findings with the HR pathway (Bristow and Hill, 2008; Chan et al., 2008), hypoxia might alter the NHEJ-associated repair of G1-associated DNA-dsbs. To test our hypothesis, we synchronized normal human fibroblasts (GM05757) in G0–G1 and measured the induction and resolution of γ-H2AX, ATM(Ser1981) and 53BP1 intranuclear foci and DNA-dsb rejoining following ionizing radiation under continual oxic, hypoxic or anoxic gas treatments. Herein, we report that hypoxic cells have a defective NHEJ pathway and acquire increased residual DNA-dsbs, as well as chromosomal aberrations, when repair is allowed to take place under continual hypoxia. Our findings are consistent with aberrant DNA-dsb sensing and repair in chronically hypoxic cells as a potential factor in hypoxia-mediated tumor progression (Bristow and Hill, 2008).

## Results

### G0–G1 synchronized fibroblasts represent a robust model to study DNA repair under continual hypoxia

To study DNA-dsb repair in hypoxic cells, we synchronized normal human fibroblasts in the G0–G1 phase before DNA damage. In this model, the exogenous DNA damage created by ionizing radiation can be studied without the bias from endogenous DNA damage created during DNA replication in the S phase of the cell cycle (Al Rashid et al., 2005). Furthermore, the induction of γ-H2AX, or other DNA damage sensor foci, which occur as a result of replicative breaks or chromatin compaction in the S and G2 phases of the cell cycle, respectively, can be avoided (Liu et al., 2008).

In this system, hypoxic (0.2% $O_2$) and anoxic (0% $O_2$) gas treatments for 16 hours led to increased activation of HIF1-α and increased expression of CAIX, VEGF and GRP94 (supplementary material Fig. S1). As previously described (Chan et al., 2008), the anoxic marker GRP94 was maximally expressed only in anoxic cells, confirming the specificity of our gassing system (supplementary material Fig. S1B).

We next examined the oxygen enhancement ratio (OER) under hypoxic and anoxic conditions in our cell system. Tumor cells and fibroblasts irradiated in the presence of air are two to three times more radio-sensitive when compared with cells irradiated under hypoxia or anoxia, because of the radiochemical principle in which a lack of oxygen leads to decreased DNA damage following exposure to ionizing radiation (Bristow and Hill, 2008; Brown and Wilson, 2004; Sprong et al., 2006). This sensitizing effect of oxygen is dependent on the intracellular oxygen concentration at the time of irradiation, and is a sensitive indicator of the degree that hypoxia or anoxia was achieved beyond simple changes in gene and protein expression. This degree of sensitization is known as the ‘oxygen enhancement ratio’, which represents the ratio of doses required for equal biological effect (a surviving fraction of 0.1) under anoxia versus oxia (Bristow and Hill, 2008). The observed OERs under hypoxia or anoxia were 1.81±0.31 and 2.02±0.13, respectively (Fig. 1A). This is consistent with the OER ranges of 1.6 to 2.6 that have been reported previously for normal human fibroblasts (Sprong et al., 2006). Using the G0–G1 cells, we also tested for hypoxia-induced apoptosis, but found no evidence of apoptosis following oxic or hypoxic gassing treatments (supplementary material Fig. S2A). Together, these data support the use of G0–G1 fibroblasts for the study of DNA repair under hypoxic conditions, given the relative lack of toxicity and lack of rapid apoptotic death over the duration of gassing treatments.

Using this model gassing system, we then examined formation of γ-H2AX foci following irradiation to determine the number of DNA-dsbs induced under oxic, hypoxic and anoxic gassing conditions. Discrete γ-H2AX foci were detected at 30 minutes following irradiation under oxic conditions (Fig. 1B). Consistent with an OER of 1.81–2.02, the number of γ-H2AX foci per nucleus decreased significantly under hypoxic and anoxic conditions. We conclude that the induction of γ-H2AX foci following irradiation is dependent on oxygen in G0–G1 fibroblasts.

Previous studies have reported that the ATM and ATR kinases are activated under severe hypoxia or anoxia (<0.1% $O_2$) (Bencokova et al., 2009; Freiberg et al., 2006; Gibson et al., 2005; Hammond et al., 2004). This could bias the use of γ-H2AX as a biomarker of exogenous DNA-dsbs under hypoxic conditions, given its dependence on ATM. To verify that hypoxia alone does not activate the ATM–p53–CHK2 signalling pathway in our model system, we examined the phosphorylation of these proteins following oxic or hypoxic gas treatment. Hypoxic treatment (0.2% $O_2$) alone did not lead to phosphorylation of H2AX, CHK1, CHK2 or p53 (Fig. 1C). By contrast, the ATM–p53–CHK2 pathway remained intact in G0–G1 cells under hypoxia as it was activated in response to exogenous DNA damage. Furthermore, unlike prolonged hypoxic exposures (e.g. 48–72 hours), we did not detect a change in the

levels of expression of RAD51 or KU70 protein (supplementary material Fig. S2B) (Chan et al., 2008). We conclude that the G0–G1 fibroblast model system can be used to track γ-H2AX and ATM as biomarkers of exogenous DNA-dsb induction and repair in hypoxic cells.

### Increased residual γ-H2AX foci and defective DNA-dsb repair in fibroblasts maintained under continual hypoxia

To study DNA-dsb repair under continual hypoxia, we tracked γ-H2AX foci following irradiation under oxic and hypoxic conditions. The initial number of γ-H2AX foci (detected at 30 minutes after irradiation) decreased rapidly to background levels at 24 hours after irradiation under oxic conditions (Fig. 2A). By contrast, despite a reduced initial level of γ-H2AX foci, the number of residual γ-H2AX foci per nucleus remained elevated at 24 hours under continual hypoxic gassing conditions ($P<0.05$). There was a significant decrease in the rate of loss of γ-H2AX foci under continual hypoxic conditions (0.11±0.09 foci/hour) when compared with rates under oxic conditions (1.11±0.37 foci/hour; $P=0.03$).

Under both oxic and hypoxic conditions, all nuclei were positive for γ-H2AX foci at 30 minutes after 2 Gy irradiation (Fig. 2B). However, following 24 hours of repair, more than 67% of the hypoxic cells still had γ-H2AX-positive nuclei, compared with only 19% of the oxic cells ($P<0.05$). A similar finding was apparent using γ-H2AX nuclear intensity as an endpoint (supplementary material Fig. S3A). We also confirmed these findings in human prostate (22RV1) and colorectal (HCT116) cancer cell lines. We observed an increase in residual γ-H2AX foci per nucleus and increased percentage of γ-H2AX-positive cells under hypoxia at 24 hours following irradiation (supplementary material Figs S4, S5). Western blotting confirmed elevated γ-H2AX protein levels in hypoxic cells following DNA damage (Fig. 2C). We conclude that hypoxic cells have increased residual γ-H2AX activation following exogenous DNA damage. The dose response of the data confirms that this effect is specific to the induction and repair of DNA damage and not a nonspecific effect of hypoxia per se.

The resolution of γ-H2AX following DNA damage involves dephosphorylation of the Ser139 residue by protein phosphatase 2A (PP2A) (Chowdhury et al., 2005). PP2A has been shown to dephosphorylate γ-H2AX in an ATM-, ATR- or DNA-PKcs-independent manner (Chowdhury et al., 2005). However, there was no change in PP2A expression at 24 hours following irradiation under hypoxic conditions (Fig. 2D). Therefore, increased γ-H2AX expression under continued hypoxia is independent of altered PP2A expression in hypoxic cells.

To examine whether the increased residual γ-H2AX under hypoxia is dependent on ATM, we treated cells with an inhibitor of ATM during irradiation. KU0055933 (ATM-i) is a specific inhibitor of ATM kinase and is 100 times more potent against ATM than any other phosphatidylinositol-3-like kinase (Hickson et al., 2004). We have previously shown that 10 μM ATM-i decreases the phosphorylation of ATM substrates under oxic conditions (Al Rashid et al., 2011; Fraser et al., 2011). Control

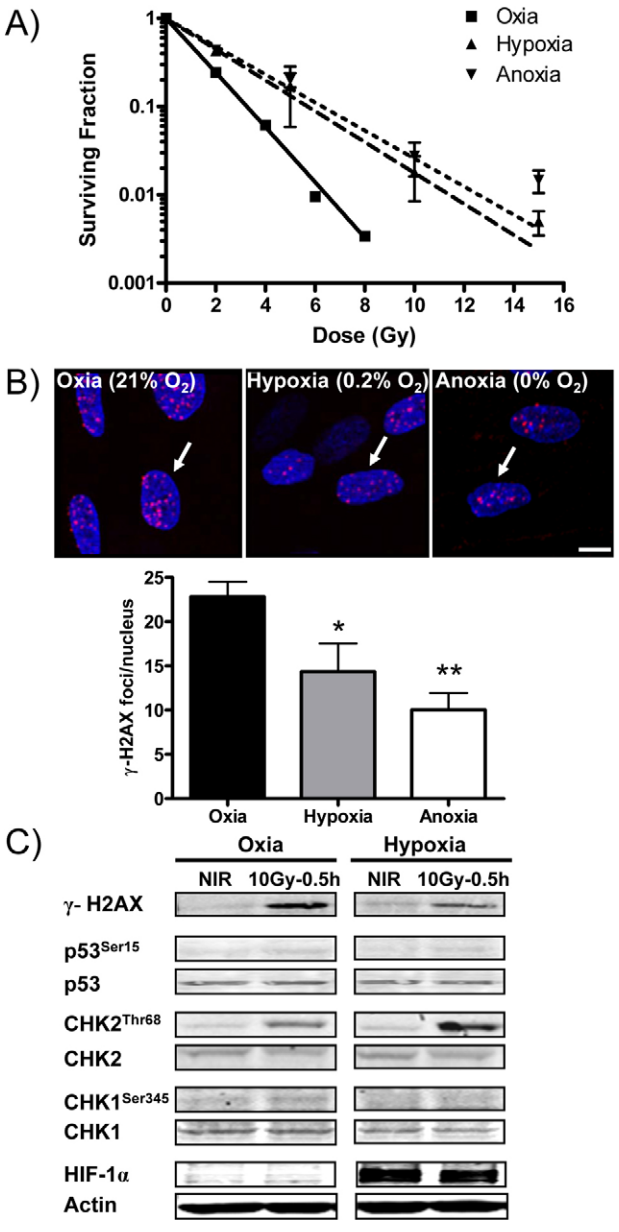


**Fig. 1. Hypoxia leads to radioresistance without activating the ATM–p53–CHK2 pathway in G0–G1 fibroblasts.** (**A**) Radiation clonogenic survival of G0–G1 fibroblasts following oxic (21% $O_2$), hypoxic (0.2% $O_2$) or anoxic (0% $O_2$) gas treatment. Cells were gassed for 16 hours and irradiated with 2, 4, 6, 8, 10 or 15 Gy. The mean survival ± s.e.m. represent data from three independent experiments. The data were modeled to the linear-quadratic equation of cell survival as previously described (Liu et al., 2008). (**B**) Representative confocal images of G0–G1 fibroblasts irradiated with 2 Gy and stained for γ-H2AX (red) at 30 minutes under 16 hours of continual oxic (21% $O_2$), hypoxic (0.2% $O_2$) or anoxic (0% $O_2$) treatment. Cells were counterstained with DAPI (blue) for nuclear DNA. Scale bar: 10 μm. Shown is the quantification of γ-H2AX foci per nucleus under continual oxia, hypoxia or anoxia following 2 Gy. The mean number of γ-H2AX foci ± s.e.m. represent data from three to five independent experiments. Asterisks denote significant difference between oxic control and hypoxic treatment (*$P<0.05$) or anoxic treatment (**$P<0.05$). (**C**) Western blot to test for activation of ATM or ATR kinase activity under hypoxia or exogenous DNA damage in G0–G1 fibroblasts. Western blots show protein expression of γ-H2AX, total p53, p53(Ser15), total CHK1, CHK1(Ser345), total CHK2 and CHK2(Thr68) in G0–G1 fibroblasts following 16 hours of oxic (21% $O_2$) or hypoxic (0.2% $O_2$) gas treatment with or without 10 Gy of irradiation. HIF-1α and actin protein expression are also shown as hypoxia and loading controls, respectively.

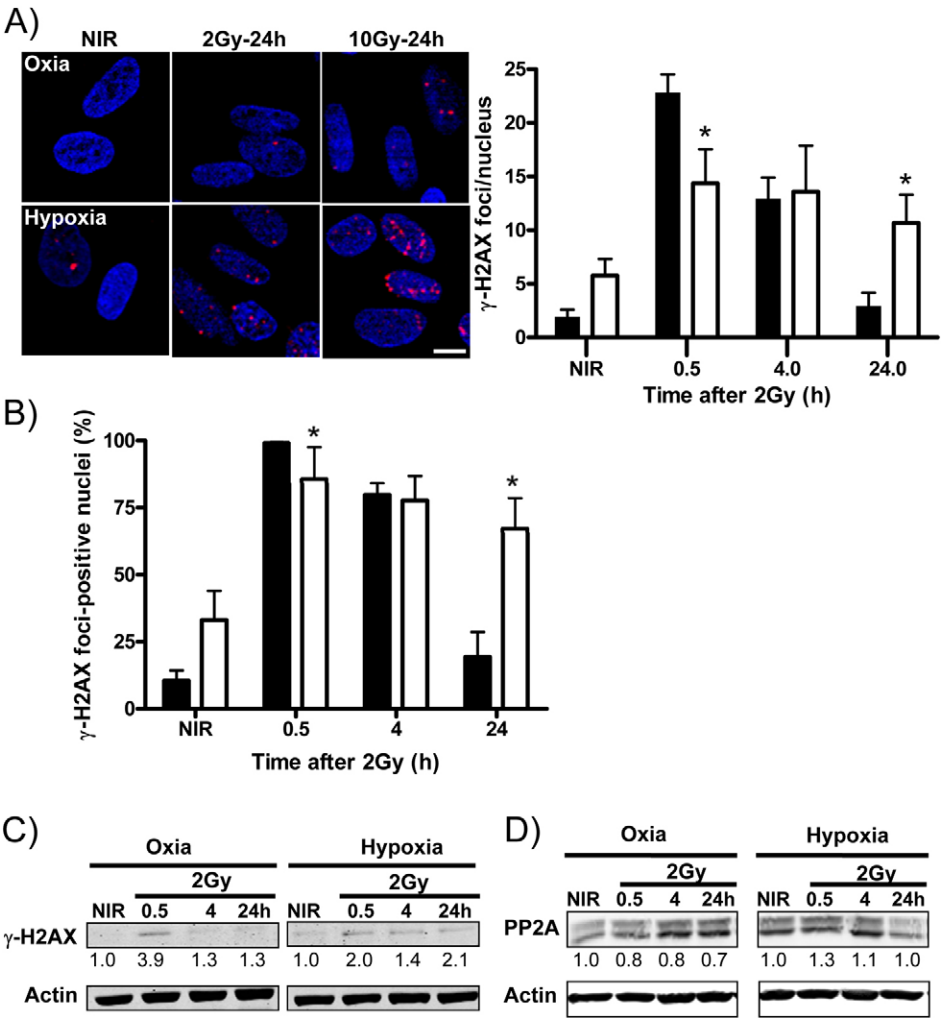


**Fig. 2. Increased residual γ-H2AX foci in cells repairing under continual hypoxia.** (**A**) Left panel shows confocal images of G0–G1 fibroblasts stained for γ-H2AX (red) and counterstained with DAPI (blue) at 24 hours of continual oxic (21% $O_2$) or hypoxic (0.2% $O_2$) gassing and following 2 or 10 Gy irradiation and 16 hours of pre-gassing. Scale bar: 10 μm. Right panel shows the mean number of γ-H2AX foci per nucleus ± s.e.m. following 2 Gy irradiation at 30 minutes, 4 hours or 24 hours of continual oxic (21% $O_2$) or hypoxic (0.2% $O_2$) gassing. Data are from five independent experiments. The asterisk denotes a significant difference between oxic control and hypoxic treatment (*$P<0.05$). Black columns, oxia; white columns, hypoxia. (**B**) The mean number of γ-H2AX foci-positive cells (± s.e.m.; nuclei with five or more γ-H2AX foci) plotted as a function of time following 2 Gy of irradiation under oxic (black columns) and hypoxic (white columns) conditions. Data are based on five independent experiments. The asterisk denotes a significant difference between oxic control and hypoxic treatment (*$P<0.05$). (**C**) Western blot for γ-H2AX protein expression at 30 minutes, 4 hours or 24 hours post 2 Gy irradiation under continued oxic (21% $O_2$) or hypoxic (0.2% $O_2$) gas treatment. (**D**) Western blot for PP2A protein expression at 30 minutes, 4 hours or 24 hours of continual oxic (21% $O_2$) or hypoxic (0.2% $O_2$) gassing following 2 Gy irradiation.

experiments showed that treatment with ATM-i decreased ATM(Ser1981) and γ-H2AX foci at 30 minutes following 2 Gy irradiation under both oxic and hypoxic conditions (supplementary material Figs S6, S7). The residual γ-H2AX foci at 24 hours following irradiation under continual hypoxic condition were also decreased following ATM-i treatment (supplementary material Fig. S7). We conclude that the residual γ-H2AX signal under hypoxia is, in part, dependent on ATM.

### Increased residual foci of 53BP1 and ATM(Ser1981) under hypoxia

To confirm whether residual γ-H2AX expression is associated with the altered retention of DNA damage sensors 53BP1 and ATM(Ser1981), we examined induction and resolution of 53BP1 and ATM(Ser1981) foci under hypoxia. The number of initial 53BP1 foci at 30 minutes following 2 Gy irradiation was decreased under hypoxia, which is consistent with the hypoxic γ-H2AX response. Yet, hypoxic cells also retained increased 53BP1 foci at 24 hours ($P<0.05$) (Fig. 3A). We also examined residual 53BP1 foci in asynchronously growing fibroblasts and observed a similar pattern whereby hypoxic cells retained increased 53BP1 foci for up to 72 hours following irradiation (data not shown). There was no change in 53BP1 protein expression in hypoxic cells. This is consistent with a change in subnuclear localization of 53BP1, rather than a change in expression, following hypoxic exposure (Fig. 3B). Similarly, the residual number of ATM(Ser1981) foci and ATM(Ser1981) nuclear intensity also remained elevated under hypoxia ($P=0.26$ and $P=0.37$, respectively) (Fig. 3C, supplementary material Fig. S3B). We conclude that DNA repair is compromised under continual hypoxic exposure, leading to increased retention of the DNA-dsb-sensing proteins γ-H2AX, 53BP1 and ATM(Ser1981).

### Increased residual γ-H2AX foci under hypoxia represent DNA-dsbs

To test whether retained DNA repair foci represent non-repaired DNA-dsbs, we performed neutral comet assays. As expected, the initial number of DNA-dsbs was decreased in irradiated hypoxic cells ($P<0.05$) (Fig. 4A). However, there was an increase in residual DNA-dsbs under hypoxic conditions at 24 hours following 30 Gy ($P=0.29$). The residual breaks were maintained up to 48 hours following 30 Gy irradiation under hypoxic conditions (supplementary material Fig. S8A). Similarly to our foci data at lower doses, despite a decreased number of initial DNA-dsbs, hypoxic cells retained increased residual DNA-dsbs. We also examined the effect of inhibiting ATM and DNA-PKcs kinases on residual DNA-dsbs under oxic and hypoxic conditions. We treated cells with specific inhibitors of ATM (KU0055933;

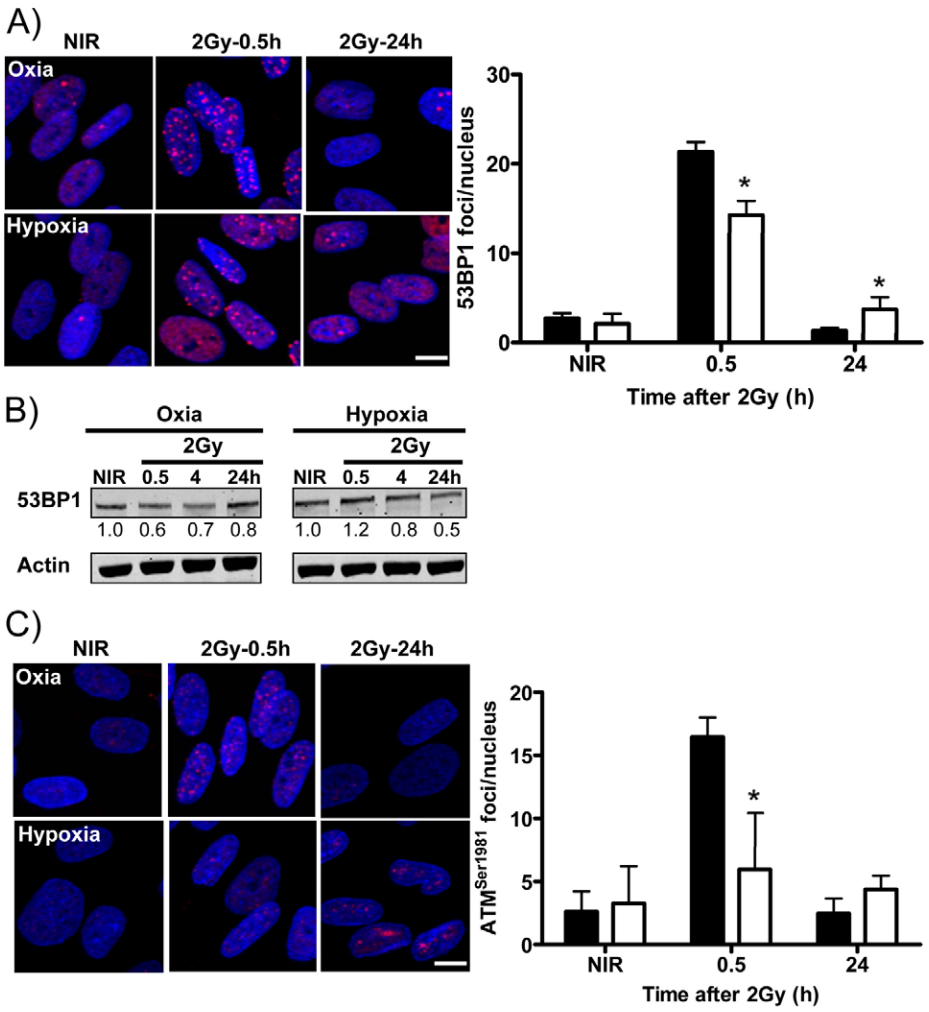


**Fig. 3. Increased residual 53BP1 and ATM(Ser1981) foci in hypoxic cells.** (**A**) Left panel shows representative confocal images of G0–G1 fibroblasts irradiated with 2 Gy and stained for 53BP1 (red) after 30 minutes or 24 hours under continual oxic (21% $O_2$) or hypoxic (0.2% $O_2$) gassing following 16 hours of pre-gassing. Right panel shows the quantification of 53BP1 foci per nucleus following similar treatment. The mean number of 53BP1 foci ± s.e.m. represent data from five independent experiments. The asterisk denotes a significant difference between oxic control and hypoxic treatment (*$P$<0.05). (**B**) Western blot for 53BP1 protein expression at 30 minutes, 4 hours or 24 hours following 2 Gy under continual oxic (21% $O_2$) or hypoxic (0.2% $O_2$) gassing following 16 hours of pre-gassing. (**C**) Left panel shows confocal images of G0–G1 fibroblasts stained for ATM(Ser1981) (red) and counterstained with DAPI (blue) after 30 minutes or 24 hours following 2 Gy under oxic (21% $O_2$) or hypoxic (0.2% $O_2$) gassing and following 16 hours of pre-gassing. Right panel shows the quantification of ATM(Ser1981) foci per nucleus for the same treatment. The mean ATM(Ser1981) foci ± s.e.m. represent data from two independent experiments. Asterisks denote significant difference between oxic control and hypoxic treatment (*$P$<0.05). Black columns, oxia; white columns, hypoxia. Scale bars: 10 μm.

ATM-i) and DNA-PKcs (KU0057788; DNA-PK-i) during irradiation. The number of residual DNA-dsbs was further increased under hypoxic conditions with ATM-i and DNA-PK-i treatment (Fig. 4B). The residual breaks were maintained up to 72 hours following irradiation under hypoxic conditions. Control experiments showed that hypoxia alone does not induce DNA-dsbs for up to 88 hours of continual gassing (supplementary material Fig. S8B). We also determined the relative repair of DNA single-strand breaks (DNA-ssbs) and base damage under oxic and hypoxic conditions using the alkaline comet assay (supplementary material Fig. S9). As expected, the initial amount of damage was decreased in hypoxic G0–G1 fibroblasts when compared with levels in oxic cells. However, there was no detectable increase in residual DNA-ssbs or base damage at 24 hours following 10 Gy irradiation in hypoxic versus oxic cells. We conclude that there is a defect in rejoining of DNA-dsbs in hypoxic G0–G1 fibroblasts relative to oxic G0–G1 fibroblasts.

### Residual DNA-dsbs under continual hypoxia lead to decreased clonogenic survival

We next wished to determine the consequences of the observed hypoxia-mediated residual DNA-dsbs on clonogenic cell survival. In our system, hypoxic (0.2% $O_2$) gassing treatment did not significantly decrease cell proliferation for up to 72 hours (Fig. 5A). Hypoxic gassing treatment also did not significantly decrease cell survival in G0–G1 fibroblasts upon reoxygenation during colony formation (Fig. 5B). By contrast, clonogenic survival was decreased to 6% when cells were kept under continual hypoxia for a period of 15 days for colony formation. Anoxic gassing treatment significantly decreased survival by more than 31% ($P$<0.05). The clonogenic survival of oxic cells following 2 Gy irradiation and 30 minutes of repair was reduced to 40% (Fig. 5C). Consistent with the OER, the surviving fraction of hypoxic and anoxic G0–G1 cells was increased at ~80%, following a similar 2 Gy dose.

We then examined the survival of G0–G1 fibroblasts irradiated under oxic, hypoxic or anoxic conditions as a function of continual gassing and 30 minutes or 24 hours of repair before trypsinization and potential proliferation. This tests for the ability of cells to repair potentially lethal damage (PLDR) under non-proliferating conditions prior to replating. PLDR is defined as the enhancement in survival when cells are held in a quiescent phase for several hours following irradiation, relative to proliferating cells (Weichselbaum et al., 1983). There was a 20% enhancement in the absolute survival at 24 hours under oxic conditions in G0–G1 cells. We also observed a 30% increase in surviving fraction of hypoxic cells at 24 hours. Anoxic cells showed no evidence of increased survival. We conclude that hypoxia-associated residual

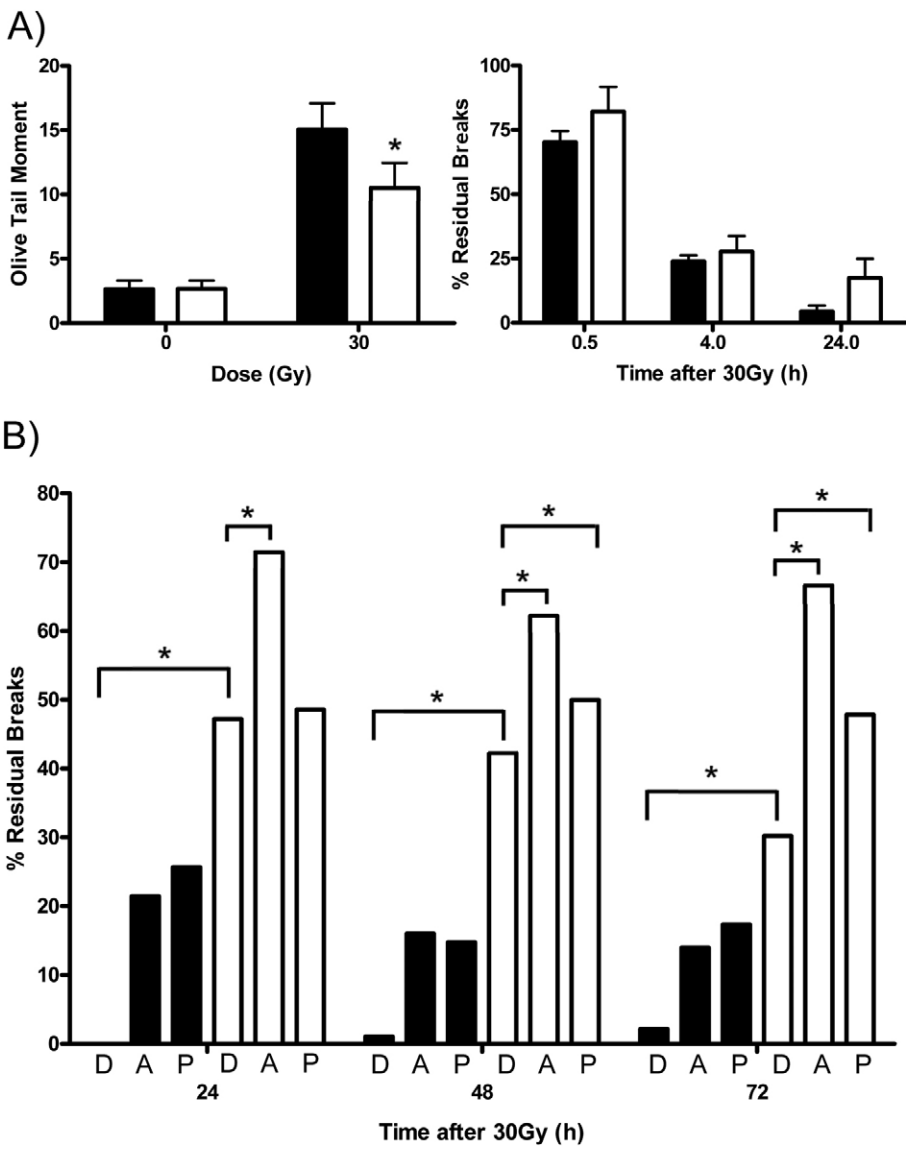


**Fig. 4. DNA-dsb rejoining under continued hypoxia.** (**A**) Neutral comet assay of DNA-dsb rejoining in G0–G1 fibroblasts. Left panel shows initial DNA-dsbs following 30 Gy irradiation in oxic (black columns) versus hypoxic (white columns) cells. The mean olive tail moment (OTM) values ± s.e.m. represent data from four independent experiments. Right panel shows DNA-dsb rejoining kinetics at 0–24 hours under oxic (black columns) or hypoxic (white columns) gassing. (**B**) DNA-dsb rejoining kinetics at 24–72 hours under oxic or hypoxic gassing following 16 hours of pre-gassing. Cells were treated with ATM-i (KU0055933, 10 μM), DNA-PK-i (KU0057788, 4 μM) or vehicle alone (DMSO) for 1 hour prior to irradiation. D, DMSO; A, ATM-i; P, DNA-PKi. Black columns, oxia; white columns, hypoxia.

DNA-dsbs are not lethal to G0–G1 fibroblasts when they are re-oxygenated during colony formation. We also examined the survival of G0–G1 fibroblasts that had been irradiated and kept under continual hypoxic conditions for the duration of colony formation. The absolute survival was decreased to 36% at 24 hours under continual hypoxic conditions. We conclude that the residual DNA-dsbs observed in hypoxic cells are lethal when the cells are kept under continual hypoxia for a prolonged period (i.e. up to 15 days).

### Increased chromosomal aberrations in cells maintained under continual hypoxia following exogenous damage

To examine the types of chromosomal aberration induced following ionizing radiation and continual hypoxia (for up to 100 hours), we used multicolor fluorescence in situ hybridization (M-FISH) and Giemsa staining assays. We released irradiated G0–G1 synchronized fibroblasts into the G2–M phases of the cell cycle under continual oxic (21% $O_2$) or hypoxic (0.2% $O_2$) environments and harvested cells at first mitosis to score all the distinct types of chromosomal aberrations. To investigate the complex structural chromosomal abnormalities under hypoxic conditions, we performed M-FISH assays. We observed the formation of anaphase bridges in irradiated hypoxic (0.2% $O_2$) cells (Fig. 6A). Similarly to our foci and neutral comet data, we observed increased residual DNA-dsbs (chromosome breaks) in hypoxic cells (Table 1). Hypoxic cells also showed an increased incidence of chromatid breaks, fragmented DNA, ring chromosomes and telomeric fusions (Fig. 6B, Table 1). There was also an increase in the frequency of other chromosomal abnormalities, including chromosomal rearrangements, reciprocal translocations, nonreciprocal translocations and marker chromosomes in irradiated hypoxic cells (Fig. 6C, Table 1). However, hypoxic (0.2% $O_2$) gassing treatment alone did not significantly induce any chromosomal aberrations (Table 1). We conclude that there are increased residual DNA breaks under continual hypoxic conditions and this leads to the accumulation of multiple complex chromosomal rearrangements in cells maintained under chronically hypoxic environments.

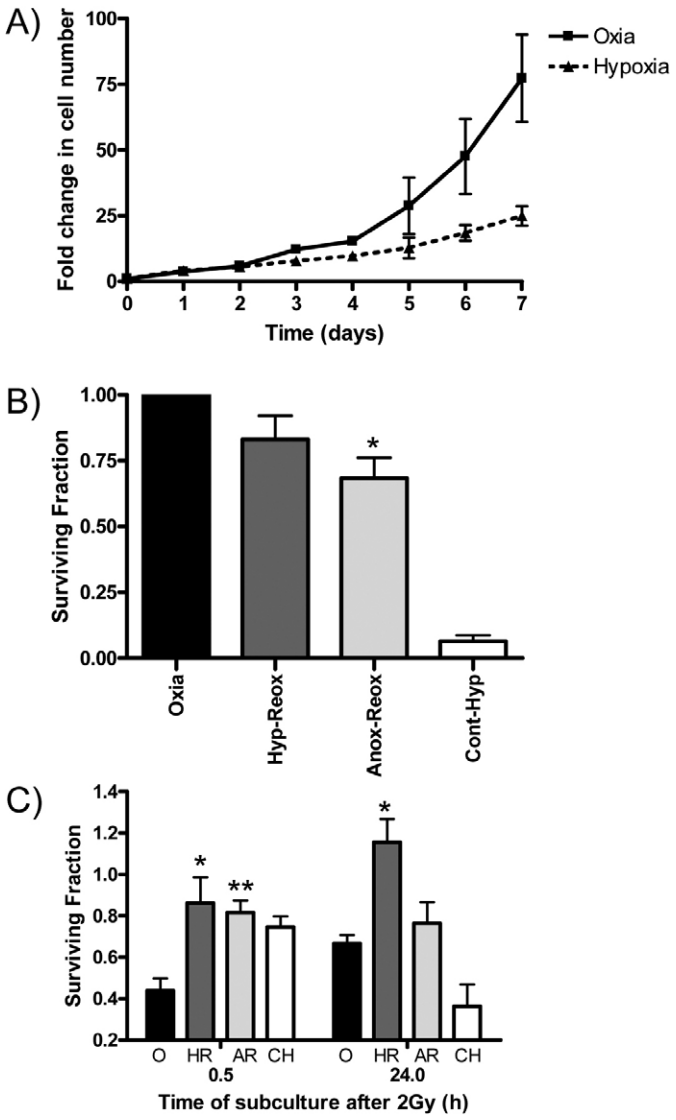


**Fig. 5. Clonogenic survival of hypoxic cells containing residual damage.** (**A**) Cell proliferation of asynchronously growing fibroblasts under oxic versus hypoxic conditions. (**B**) Clonogenic survival of G0–G1 fibroblasts following 16 hours exposure to 21% $O_2$ (oxia), 0.2% $O_2$ (hypoxia) or 0% $O_2$ (anoxia). Continual hypoxic G0–G1 fibroblasts (Cont-Hyp) were exposed to hypoxia (0.2% $O_2$) for 16 hours and plated for colony formation and kept under 0.2% $O_2$ for up to 15 days. (Shown is the mean survival ± s.e.m. and represent data from two to five independent experiments). The asterisk denotes a significant difference between oxic and anoxic cell survival (*$P$<0.05). (**C**) Radiation clonogenic survival of G0–G1 fibroblasts following 16 hours of oxic (21% $O_2$), hypoxic (0.2% $O_2$) or anoxic (0% $O_2$) pre-gassing treatment, 2 Gy of irradiation and 30 minutes or 24 hours of continual oxic (21% $O_2$), hypoxic (0.2% $O_2$) or anoxic (0% $O_2$) gas treatment prior to trypsinization and plating for colony formation. The means ± s.e.m. represent data from two to three independent experiments. Asterisks denote significant difference between oxic control and hypoxic treatment (*$P$<0.05), or anoxic treatment (**$P$<0.05). O, oxia; HR, hypoxic gassing followed by reoxygenation during colony formation; AR, anoxic gassing followed by reoxygenation during colony formation; CH, continual hypoxic gassing during colony formation.

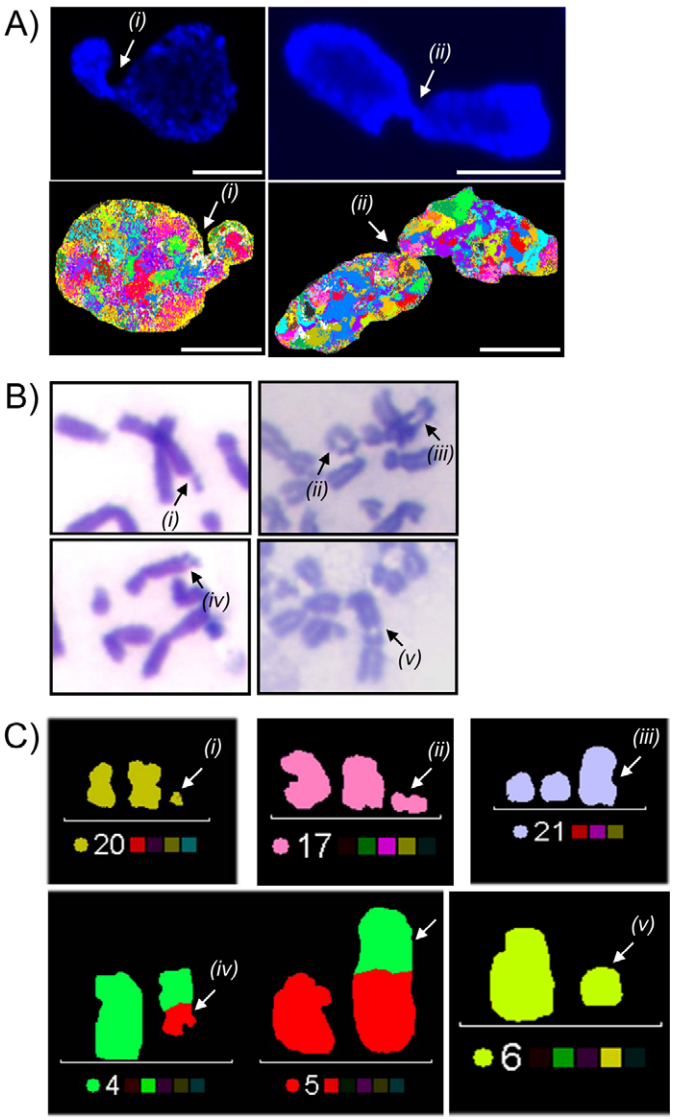


**Fig. 6. Increased chromosomal aberrations in cells repairing under continual hypoxia.** G0–G1 synchronized fibroblasts were exposed to oxic (21% $O_2$) or hypoxic (0.2% $O_2$) environments for 16 hours. The cells were then irradiated (2 Gy) and gassed continuously for post-irradiation repair period of 24 hours. The cells were then released from G0–G1 phase to enter G2–M phase. Cells were harvested by trypsinization 60 hours after release and incubation with 0.02 μg/ml of colcemid for 12 hours to collect metaphase spreads for analysis. (**A**) Chromatin bridges (i) and internuclear anaphase bridges (ii) in hypoxic cells. Top panel shows representative images of fibroblasts stained with DAPI (blue) at 84 hours of continual hypoxic (0.2% $O_2$) gassing and following 2 Gy of irradiation. Bottom panel shows representative M-FISH images of fibroblasts indicating the presence of anaphase bridges and internuclear anaphase bridges at 84 hours of continual hypoxic (0.2% $O_2$) gassing and following 2 Gy irradiation. Scale bars: 10 μm. (**B**) Representative images of partial metaphase spreads of fibroblasts stained with Giemsa at 84 hours of continual hypoxic (0.2% $O_2$) gassing and following 2 Gy irradiation. (i) chromatid break; (ii) ring chromosome; (iii) chromosome break; (iv) chromosome break; (v) telomeric fusion. (**C**) Partial M-FISH karyotype of fibroblasts at 84 hours of continual hypoxic (0.2% $O_2$) gassing and following 2 Gy of irradiation. (i) fragment derived from chromosome 20; (ii) fragment derived from chromosome 17; (iii) marker chromosome originated from chromosome 21; (iv) reciprocal translocation between chromosomes 4 and 5; (v) ring chromosome 6.

**Table 1. Chromosomal aberrations in oxic and hypoxic fibroblasts following DNA damage**

| | | Oxia NIR | Hypoxia NIR | Oxia 2Gy | Hypoxia 2Gy | Oxia 2Gy DMSO | Oxia 2Gy DNA-PKi |
|---|---|---|---|---|---|---|---|
| Giemsa | Chromosome break (%) | 0 (0) | 0 (0) | 2 (5) | 10 (25) | – | – |
| | Chromatid break (%) | 0 (0) | 2 (7) | 3 (8) | 9 (23) | – | – |
| | Accentric fragments (%) | 0 (0) | 1 (3) | 4 (10) | 8 (20) | – | – |
| | Ring chromosomes (%) | 0 (0) | 1 (3) | 0 (0) | 2 (5) | – | – |
| | Telomeric fusion (%) | 0 (0) | 0 (0) | 0 (0) | 1 (3) | – | – |
| M-FISH | Abnormal metaphases (%) | 8 (35) | 10 (33) | 26 (74) | 30 (83) | 12 (55) | 19 (79) |
| | Intrachromosomal rearrangements* (%) | 0 (0) | 2 (7) | 16 (46) | 23 (64) | 4 (18) | 17 (71) |
| | Reciprocal translocation (%) | 0 (0) | 0 (0) | 3 (9) | 6 (17) | 1 (5) | 5 (21) |
| | Nonreciprocal translocation (%) | 0 (0) | 0 (0) | 6 (17) | 9 (25) | 5 (23) | 9 (38) |
| | Accentric fragments and double minutes (%) | 0 (0) | 0 (0) | 5 (14) | 3 (8) | 0 (0) | 2 (8) |

Shown are absolute numbers and percentages (in parentheses) of chromosomal aberrations. A minimum of 30 metaphases were scored for Giemsa staining analysis. A minimum of 22 metaphases were scored for M-FISH analysis.

*Intrachromosomal rearrangements include deletions, duplications and inversions within a chromosome.

## Discussion

Acute and chronic hypoxia exists in human tumors. To our knowledge, this is the first report to track and measure DNA-dsb repair and chromosomal aberrations under continual hypoxic conditions following exogenous damage. Previous studies investigated repair during hypoxic irradiation conditions followed by reoxygenation, and concluded that the mutation rate and DNA-dsb repair rate were not influenced by hypoxia (Banath et al., 2005; Olive and Banath, 2004). We observed increased residual γ-H2AX foci in G0–G1 cells at 24 hours following irradiation under continual hypoxic conditions relative to oxic conditions. This observation was also independent of PP2A expression, cell death or cell cycle bias in quantifying γ-H2AX or other DNA repair endpoints. We also observed increased 53BP1 and ATM(Ser1981) residual foci under continual hypoxia following irradiation. We confirmed that these residual foci represent DNA-dsbs using neutral comet assays. To address how hypoxia specifically alters DNA-dsb repair, our experiments were conducted at 0.2% $O_2$, which did not activate ATM or ATR kinases. Our data suggest that despite the reduction in initial number of DNA-dsbs under hypoxia, the repair of these breaks is compromised such that residual damage can be greater than in oxic cells. This might, in part, explain the increased genetic instability observed in hypoxic cells that adapt to low oxygen conditions or reoxygenation. Whether similar differences exist between oxic and hypoxic cells in the repair of endogenous DNA-dsbs during DNA replication requires further study.

However, these residual DNA-dsbs in hypoxic cells did not lead to increased clonogenic cell death when they were reoxygenated. By contrast, cell survival was compromised when cells were kept under continual hypoxic conditions (i.e. at 0.2% $O_2$ in a controlled microenvironmental chamber) throughout the entire period of colony formation. These results suggest that the lethality of residual DNA-dsbs is linked to the duration of post-treatment hypoxia and related to the subregions of cycling versus chronic hypoxia in human tumors (Bristow and Hill, 2008).

NHEJ is the predominant DNA-dsb repair pathway in the G1 phase of the cell cycle (O'Driscoll and Jeggo, 2006). There are conflicting data in the literature regarding hypoxia-mediated decrease in NHEJ repair. Studies from our laboratory have indicated that NHEJ-related genes are variably downregulated at the mRNA and protein levels in both normal and malignant hypoxic cells (Meng et al., 2005). By contrast, Um and colleagues reported that the activity and expression of DNA-PK is increased under hypoxic (1% $O_2$) conditions (Um et al., 2004). They specifically showed that DNA-PKcs could physically interact with the HIF-1 complex and directly phosphorylate HIF-1α, resulting in its stabilization. However, neither of these studies measured DNA-dsb repair in chronically hypoxic cells. Our data suggest that there are increased unrepaired DNA-dsbs in G0–G1 hypoxic fibroblasts following DNA damage, indicating that the NHEJ pathway might be compromised in hypoxic cells. It is currently not known how hypoxia alters NHEJ repair in other phases of the cell cycle (i.e. S and G2 phases). Our clonogenic data suggest that DNA-dsb repair is compromised in all phases of the cell cycle in hypoxic cells, leading to decreased clonogenic survival under conditions of prolonged continual hypoxia. A study by Lara and co-workers reported for the first time that hypoxia decreases the expression of Ku70 and Ku80 in clinical cervical tumors (Lara et al., 2008). However, we did not observe a change in KU70 expression in our G0–G1 fibroblast model system. Recently, it has been suggested that an alternative DNA-PKcs-independent pathway also contributes to the repair of DNA-dsbs (Wu et al., 2008). This back-up pathway is active in all phases of the cell cycle. More studies are required with different cell types to test whether hypoxia leads to a defect in both DNA-PKcs-dependent and -independent NHEJ pathways throughout the cell cycle.

Non-repaired or mis-repaired DNA-dsbs are dangerous lesions because they can lead to chromosomal aberrations and rearrangements (Jeggo and Lobrich, 2007). Coquelle and colleagues initially reported that severe hypoxia could induce fragile sites (Coquelle et al., 1998). Fragile sites are regions within chromosomes that are prone to chromosomal rearrangement and activation of the breakage–fusion–bridge cycle for gene amplification. Hypoxia has been documented to drive the fusion of double minutes into fragile sites, thereby generating homogenously staining regions (Coquelle et al., 1998). Fragile sites have been thought to be involved in DNA-dsb-induced chromosomal aberrations (Ozeri-Galai et al., 2008). Fischer and co-workers reported similar findings in which hypoxia drives the formation of double minutes, fragile sites and anaphase bridges, which can lead to the development of gene

amplifications in glioblastoma (Fischer et al., 2008). A study by Ozeri-Galai and colleagues showed that both ATM and ATR kinases are involved in regulating the stability of fragile sites (Ozeri-Galai et al., 2008). Furthermore, they have shown that the induction of fragile sites by replication stress leads to formation of DNA-dsbs and activation of ATM, ATR and γ-H2AX. However, our data on the dose responsiveness of residual γ-H2AX foci under prolonged hypoxia suggest that we are not observing foci that are related to fragile sites.

Lee and colleagues recently reported that hypoxia gradually increased the formation of sister chromatid exchanges in human peripheral lymphocytes (Lee et al., 2010). However, they did not detect any nuclear or mitochondrial microsatellite instability in human lymphocytes exposed to hypoxia. We observed increased chromosomal aberrations (chromosome breaks, chromatid breaks, fragmented DNA, ring chromosomes, telomeric fusions, reciprocal translocations and double minutes) in cells maintained under continual hypoxic conditions following exogenous damage. The clonal survival of selected hypoxic cells with chromosomal aberrations in oncogenes or tumor suppressor genes could lead to aberrant growth, ongoing chromosomal instability and aneuploidy under prolonged hypoxia (Bindra et al., 2007; Bristow and Hill, 2008; Huang et al., 2007). Together, our data suggest it is highly plausible that a functional decrease in the repair of DNA-dsbs under hypoxia can drive the observed genetic instability and mutator phenotype in hypoxic cells.

In summary, our results support the concept that hypoxia represses the repair of DNA-dsbs, and this defective DNA repair in hypoxic cells could ultimately affect genetic changes during carcinogenesis and early angiogenesis, and/or drive tumor progression leading to a mutator phenotype. Unrepaired DNA-dsbs under hypoxic conditions could then drive genetic rearrangement and genomic instability. An understanding of DNA-dsb repair defects in hypoxic cells could help target hypoxia-induced resistance within human tumors to improve current cancer treatment modalities. Indeed, we recently reported that hypoxic cells are more sensitive to PARP inhibitors in vivo and suggest that genetic instability in hypoxic cells could be offset by these contextual synthetic lethality approaches (Chan and Bristow, 2010; Chan et al., 2010).

## Materials and Methods

### Cell culture, hypoxic gassing and irradiation treatment

The primary human fibroblast strain GM05757 was obtained from the Coriell Cell Repository and grown in 15% fetal calf serum (FCS) and α-Modified Eagle's Medium (α-MEM). Cell cultures were incubated in 5% $CO_2$ at 37℃. A synchronization protocol, as described by Little and colleagues (Little et al., 2002), was used to obtain density-inhibited G0–G1 phase cultures for studying DNA damage responses without S-phase or G2–M bias. For hypoxia studies, G0–G1 synchronized fibroblasts grown in T75 flasks were flushed with either 0% $O_2$ (anoxia), 0.2% $O_2$ (hypoxia) or 21% $O_2$ (oxia) with 5% $CO_2$ and balanced with $N_2$ for 16 hours, using a glass manifold system as described previously (Chan et al., 2008). In some experiments, cells grown in T75 flasks were exposed to hypoxic environments (0.2% $O_2$) for 16 hours using an Invivo$_2$ 400 chamber (Ruskinn Technology Limited).

To induce exogenous DNA damage, cells were irradiated using a $^{137}Cs$ irradiator (MDS Nordion), as previously described (Chan et al., 2008). They were then gassed continuously for post-irradiation repair periods of 30 minutes, 4 hours or 24 hours at 37℃ and assayed for residual DNA damage. In some experiments, cells were incubated with the ATM inhibitor KU0055933 (10 μM in DMSO; AstraZeneca) or DNA-PKcs inhibitor KU0057788 (4 μM in DMSO; AstraZeneca) for 1 hour before irradiation. Control cultures were incubated with carrier DMSO alone for a similar duration.

### Western blot analysis

Protein expression was detected using western blot analysis as previously described (Meng et al., 2005). Whole-cell lysates (60–90 μg) were loaded and separated on 4–12% Tris–Glycine gels (Invitrogen). Gels were then transferred onto nitrocellulose membranes and blocked using LI-COR blocking buffer (LI-COR Biosciences) and incubated with appropriate primary and secondary antibodies conjugated to Alexa Fluor 680 (Invitrogen) or IRdye-800 (Rockland Immunochemicals) diluted 1:20,000 in LI-COR blocking buffer (Liu et al., 2008).

Primary antibodies were used at the following dilutions: HIF-1α (BD Transduction Laboratories) 1:500; Actin (Sigma) 1:100,000; γ-H2AX (1:8000), CHK2 (1:1000) and PP2A (1:20,000) (all from Upstate Biotechnology); p53 (1:3000), CHK1 (1:1000), RAD51 (1:1000) and KU70 (1:20,000) (all from Santa Cruz Biotechnology); p53(Ser15) (1:1000), CHK2(Thr68) (1:1000) and CHK1(Ser345) (1:1000) (all from Cell Signaling Technology) and 53BP1 (Alexis Biochemicals) 1:10,000.

### RNA extraction and real-time quantitative PCR

Total RNA was extracted using TRI Reagent (Sigma) as previously described (Meng et al., 2005). Sample RNA was treated with DNase I (Invitrogen) to eliminate potential DNA contamination. The products were then reverse transcribed using Invitrogen SuperScript III Transcriptase and random hexamer primers. cDNA was then amplified for hypoxia-mediated target genes *VEGF* and *GRP94* using ABI TaqMan Gene Expression Assays and TaqMan Universal PCR Master Mix (Applied Biosystems); ribosomal 18S was used as an endogenous control. PCR was run using Stratagene Mx3005p Realtime PCR system under the control of SDS software. The fluorescence intensity threshold was set at 0.2 and the reaction cycle-threshold was obtained. Analysis was performed using the comparative $C_T$ quantification method.

### Cell proliferation, clonogenic survival and apoptotic assays

Asynchronously growing fibroblasts were exposed to hypoxic environments (0.2% $O_2$) using an Invivo$_2$ 400 chamber (Ruskinn Technology Limited). Relative cell proliferation was determined by daily counts of cells for up to 7 days during gas treatment and the data were plotted after normalizing against cell number at day 0. Clonogenic survival assays were performed as previously described (Bromfield et al., 2003). Briefly, G0–G1 contact-inhibited fibroblasts were gassed with either 0% $O_2$ (anoxia), 0.2% $O_2$ (hypoxia) or 21% $O_2$ (oxia) with 5% $CO_2$ and balanced with $N_2$ for 16 hours, irradiated and plated for colony formation. To determine the repair of potentially lethal damage (PLDR), non-proliferating G0–G1 cells were continually gassed for 30 minutes, 4 or 24 hours after irradiation and then plated for colony formation. For chronic hypoxia, the cells were irradiated, plated for colony formation and kept under 0.2% $O_2$ (hypoxia) for up to 15 days. The cells were fixed and stained with 1% Methylene Blue in 50% ethanol after 10–15 days of incubation. Colonies consisting of 50 or more cells were scored and survival was calculated based on colony formation in irradiated and non-irradiated cultures, as previously described (Chan et al., 2008). The surviving fraction for each gassing condition was normalized to the surviving fraction under oxic conditions in non-irradiated cultures. The surviving fraction for each irradiated time point was normalized to the surviving fraction of the respective non-irradiated gassing conditions. Oxygen enhancement ratios (OERs) were calculated by dividing the radiation dose for hypoxic (or anoxic) cells by the radiation dose for control oxic cells required to give a surviving fraction of 0.1. For apoptotic assays, cells were grown on coverslips inside T75 flasks and immunofluorescence analysis was performed as previously described (see below) (Al Rashid et al., 2005). Cells were stained with cleaved caspase-3 (Cell Signaling Technology) and scored using an Olympus IX81 inverted spinning-disk microscope as previously described (Liu et al., 2008). Rat1-Myc cells, which constitutively express Myc (a generous gift from Linda Penn, University of Toronto), were used as a positive control for radiation-induced apoptosis, as previously described (Bromfield et al., 2003).

### Immunofluorescence and confocal microscopy

Cells for analyses of microscopic DNA repair foci were grown on coverslips inside T75 flasks. Briefly, sterilized coverslips ware inserted into T75 flasks. The primary human fibroblast strain GM05757 was seeded in the flask. The cells were allowed to reach confluence inside the flask. The culture medium was changed at 24 hours and 48 hours after the cells reached confluence. The experiment started 48 hours following the final medium change (Little and Nagasawa, 1985). The flasks were then gassed for 16 hours, irradiated and gassed again for a repair period of 30 minutes, 4 hours or 24 hours. The coverslips were removed at appropriate time points and fixed and stained in 6 well dishes. The cells were fixed with 2% paraformaldehyde and 0.2% Triton X-100 (pH 8.2) and permeabilized with 0.5% NP40. The cells were then incubated with appropriate primary and fluorophore-conjugated secondary antibodies [Cy3 (Jackson ImmunoResearch) 1:200 and Alexa Fluor 488 (Invitrogen) 1:500] diluted in 3% BSA. Cells were counterstained with 4′,6-diamidino-2-phenylindole (DAPI) for nuclear DNA. Finally, the coverslips were mounted with Vectashield antifade solution (Vector Laboratories) before microscopy.

A Zeiss LSM510 meta two-photon microscope at a final magnification of ×400 was used to acquire confocal z-stack images consisting of 0.5 μm sections. Maximum intensity projections of the *z*-stacks were then created using Image Pro Plus software to quantify nuclear intensity (total intensity of staining), foci per

nucleus and cells positive for foci. Nuclei with five or more foci were scored as foci-positive nuclei based on background number of foci in untreated cells. A minimum of 50 nuclei were analysed for each treatment group.

Primary antibodies were used at the following dilutions: γ-H2AX (Upstate Biotechnology) 1:800; cleaved caspase-3 (Cell Signaling Technology) 1:400; ATM(Ser1981) (Rockland Immunochemicals) 1:300; and 53BP1 (Alexis Biochemicals) 1:500.

### Comet assay

To determine initial and residual DNA-dsbs, neutral comet assays were performed as previously described (Fan et al., 2004). Single-cell suspensions were mixed with 0.7% low melting agarose and spread on slides pre-coated with 1% normal melting agarose. Slides were then treated with lysis solution (2.5 mM NaCl, 100 mM EDTA, 10 mM Trizma base, 10% DMSO and 1% Triton X-100, pH 9.0) for 72 hours. The slides were prepared for electrophoresis in Tris-buffer with boric acid and EDTA for 30 minutes at 32 V. After electrophoresis, slides were air-dried and stained with 2 μg/ml of ethidium bromide and scored using KOMET 5.0 software (Kinetic Imaging). One hundred cells were scored at random for each slide and the Olive Tail Moment (% DNA in the tail/distance between centre of gravity of head and tail) was reported as a measure of DNA-dsbs, as previously described (Fan et al., 2004).

### Multicolor fluorescence in situ hybridization and chromosomal aberration assays

To determine the frequency of chromosomal aberrations, G0–G1 synchronized fibroblasts grown in T75 flasks were exposed to oxic (21% $O_2$) or hypoxic environments (0.2% $O_2$) using an Invivo$_2$ 400 chamber (Ruskinn Technology Limited) for 16 hours. Cells were then irradiated (2 Gy) using a $^{137}$Cs irradiator (MDS Nordion). They were then gassed continuously for post-irradiation repair period of 24 hours and released from G0–G1 phase to enter G2–M phase. Cells were harvested by trypsinization 60 hours after release and incubation with 0.02 μg/ml of colcemid (Invitrogen) for 12 hours. Cells were then treated with 0.075 M potassium chloride hypotonic solution for 18 minutes and fixed in methanol and acetic acid (3:1) solution to collect metaphase spreads for analysis. In some experiments, asynchronously growing fibroblasts were incubated with the DNA-PKcs inhibitor KU0057788 (1 μM in DMSO; AstraZeneca) for 1 hour before irradiation. Control cultures were incubated with carrier DMSO alone for a similar duration. Cells were harvested by trypsinization 84 hours following irradiation and incubation with 0.02 μg/ml of colcemid for 12 hours to collect metaphase spreads for analysis. For chromosomal aberrations, slides were stained with Giemsa (Invitrogen) and at least 30 metaphases were analyzed for each treatment. M-FISH analysis was performed according to the manufacturer's protocols (MetaSystems). Briefly, slides were pretreated in 2× SSC (saline-sodium citrate buffer) for 30 minutes at 70℃ and denatured in 0.07 N NaOH for 1 minute at room temperature. Probe cocktail was denatured for 5 minutes at 75℃. Following 2 days of hybridization, washing steps were performed and the slides were counterstained with DAPI. A minimum of 22 metaphases were analyzed using a Zeiss Imager M1 microscope (Carl Zeiss Canada Limited) equipped with the appropriate filters (DAPI, FITC, Spectrum Orange, TRITC, Cy5, DEAC) and the JAI CV-M4+CL progressive scan monochrome camera (JAI Inc.) and the MetaSystems Isis FISH Imaging software programs v5.3 (MetaSystems).

### Statistical analyses

Quantitative immunofluorescence data from each independent experiment was modelled using a generalized estimating equation (GEE) with a Poisson distribution in the R software program (R Foundation) (Hardin and Hilbe, 2003). In this model, all the individual values were used and the inherent dependence between the counts within the same experiment was controlled by considering each experiment as a cluster in the model as previously described (Christensen et al., 2009; Jackman et al., 2011; Kaspler et al., 2009; Liang and Zeger, 1986; Marconi et al., 2011; Revai et al., 2009). Comet data from each experiment was modelled using the GEE with a Gaussian distribution. A square root transformation was employed to stabilize the variance. Clonogenic survival was calculated as a fraction, therefore the data was analysed the data using two-tailed unpaired *t*-test or one-way analysis of variance (ANOVA) within the GraphPad Prism 4.0 software (GraphPad). For all analyses, $P<0.05$ was considered significant.

## Acknowledgements

We thank Norman Chan and Aleem Abdulla for helpful discussions and technical assistance and Richard Hill, Anne Koch, Lea Harrington and Peggy Olive for critical comments. KU0055933 and KU0057788 were generously provided by Mark O'Connor (AstraZeneca).

## Funding

The studies were supported by grants from the Terry Fox Foundation-NCIC Hypoxia PMH Program Grant [grant number 15004] and a NCIC operating grant [grant number 17154]; and also, in part, by the Ontario Ministry of Health and Long Term Care. The views expressed do not necessarily reflect those of the OMOHLT. R.K. is a holder of a CIHR-EIRR21st Studentship Award. R.G.B. is a Canadian Cancer Society Research Scientist.

Supplementary material available online at
http://jcs.biologists.org/lookup/suppl/doi:10.1242/jcs.092262/-/DC1

## References

**Al Rashid, S. T., Dellaire, G., Cuddihy, A., Jalali, F., Vaid, M., Coackley, C., Folkard, M., Xu, Y., Chen, B. P., Chen, D. J. et al.** (2005). Evidence for the direct binding of phosphorylated p53 to sites of DNA breaks in vivo. *Cancer Res.* **65**, 10810-10821.

**Al Rashid, S. T., Harding, S. M., Law, C., Coackley, C. and Bristow, R. G.** (2011). Protein-protein interactions occur between p53 phosphoforms and ATM and 53BP1 at sites of exogenous DNA damage. *Radiat. Res.* **175**, 588-598.

**Banath, J. P., Sinnott, L., Larrivee, B., MacPhail, S. H. and Olive, P. L.** (2005). Growth of V79 cells as xenograft tumors promotes multicellular resistance but does not increase spontaneous or radiation-induced mutant frequency. *Radiat. Res.* **164**, 733-744.

**Bencokova, Z., Kaufmann, M. R., Pires, I. M., Lecane, P. S., Giaccia, A. J. and Hammond, E. M.** (2009). ATM activation and signaling under hypoxic conditions. *Mol. Cell. Biol.* **29**, 526-537.

**Bindra, R. S., Schaffer, P. J., Meng, A., Woo, J., Maseide, K., Roth, M. E., Lizardi, P., Hedley, D. W., Bristow, R. G. and Glazer, P. M.** (2004). Down-regulation of Rad51 and decreased homologous recombination in hypoxic cancer cells. *Mol. Cell. Biol.* **24**, 8504-8518.

**Bindra, R. S., Gibson, S. L., Meng, A., Westermark, U., Jasin, M., Pierce, A. J., Bristow, R. G., Classon, M. K. and Glazer, P. M.** (2005). Hypoxia-induced down-regulation of BRCA1 expression by E2Fs. *Cancer Res.* **65**, 11597-11604.

**Bindra, R. S., Crosby, M. E. and Glazer, P. M.** (2007). Regulation of DNA repair in hypoxic cancer cells. *Cancer Metastasis Rev.* **26**, 249-260.

**Bristow, R. G. and Hill, R. P.** (2008). Hypoxia and metabolism. Hypoxia, DNA repair and genetic instability. *Nat. Rev. Cancer* **8**, 180-192.

**Bromfield, G. P., Meng, A., Warde, P. and Bristow, R. G.** (2003). Cell death in irradiated prostate epithelial cells: role of apoptotic and clonogenic cell kill. *Prostate Cancer Prostatic Dis.* **6**, 73-85.

**Brown, J. M. and Wilson, W. R.** (2004). Exploiting tumour hypoxia in cancer treatment. *Nat. Rev. Cancer* **4**, 437-447.

**Celeste, A., Fernandez-Capetillo, O., Kruhlak, M. J., Pilch, D. R., Staudt, D. W., Lee, A., Bonner, R. F., Bonner, W. M. and Nussenzweig, A.** (2003). Histone H2AX phosphorylation is dispensable for the initial recognition of DNA breaks. *Nat. Cell Biol.* **5**, 675-679.

**Chan, N. and Bristow, R. G.** (2010). "Contextual" synthetic lethality and/or loss of heterozygosity: tumor hypoxia and modification of DNA repair. *Clin. Cancer Res.* **16**, 4553-4560.

**Chan, N., Koritzinsky, M., Zhao, H., Bindra, R., Glazer, P. M., Powell, S., Belmaaza, A., Wouters, B. and Bristow, R. G.** (2008). Chronic hypoxia decreases synthesis of homologous recombination proteins to offset chemoresistance and radioresistance. *Cancer Res.* **68**, 605-614.

**Chan, N., Pires, I. M., Bencokova, Z., Coackley, C., Luoto, K. R., Bhogal, N., Lakshman, M., Gottipati, P., Oliver, F. J., Helleday, T. et al.** (2010). Contextual synthetic lethality of cancer cell kill based on the tumor microenvironment. *Cancer Res.* **70**, 8045-8054.

**Chowdhury, D., Keogh, M. C., Ishii, H., Peterson, C. L., Buratowski, S. and Lieberman, J.** (2005). gamma-H2AX dephosphorylation by protein phosphatase 2A facilitates DNA double-strand break repair. *Mol. Cell* **20**, 801-809.

**Christensen, E., Pintilie, M., Evans, K. R., Lenarduzzi, M., Menard, C., Catton, C. N., Diamandis, E. P. and Bristow, R. G.** (2009). Longitudinal cytokine expression during IMRT for prostate cancer and acute treatment toxicity. *Clin. Cancer Res.* **15**, 5576-5583.

**Coquelle, A., Toledo, F., Stern, S., Bieth, A. and Debatisse, M.** (1998). A new role for hypoxia in tumor progression: induction of fragile site triggering genomic rearrangements and formation of complex DMs and HSRs. *Mol. Cell* **2**, 259-265.

**Falck, J., Coates, J. and Jackson, S. P.** (2005). Conserved modes of recruitment of ATM, ATR and DNA-PKcs to sites of DNA damage. *Nature* **434**, 605-611.

**Fan, R., Kumaravel, T. S., Jalali, F., Marrano, P., Squire, J. A. and Bristow, R. G.** (2004). Defective DNA strand break repair after DNA damage in prostate cancer cells: implications for genetic instability and prostate cancer progression. *Cancer Res.* **64**, 8526-8533.

**Fischer, U., Radermacher, J., Mayer, J., Mehraein, Y. and Meese, E.** (2008). Tumor hypoxia: Impact on gene amplification in glioblastoma. *Int. J. Oncol.* **33**, 509-515.

**Fraser, M., Harding, S. M., Zhao, H., Coackley, C., Durocher, D. and Bristow, R. G.** (2011). MRE11 promotes AKT phosphorylation in direct response to DNA double-strand breaks. *Cell Cycle* **10**, 2218-2232.

**Freiberg, R. A., Hammond, E. M., Dorie, M. J., Welford, S. M. and Giaccia, A. J.** (2006). DNA damage during reoxygenation elicits a Chk2-dependent checkpoint response. *Mol. Cell. Biol.* **26**, 1598-1609.

**Gibson, S. L., Bindra, R. S. and Glazer, P. M.** (2005). Hypoxia-induced phosphorylation of Chk2 in an ataxia telangiectasia mutated-dependent manner. *Cancer Res.* **65**, 10734-10741.

**Hammond, E. M., Dorie, M. J. and Giaccia, A. J.** (2003). ATR/ATM targets are phosphorylated by ATR in response to hypoxia and ATM in response to reoxygenation. *J. Biol. Chem.* **278**, 12207-12213.

**Hammond, E. M., Dorie, M. J. and Giaccia, A. J.** (2004). Inhibition of ATR leads to increased sensitivity to hypoxia/reoxygenation. *Cancer Res.* **64**, 6556-6562.

**Hardin, J. W. and Hilbe, J.** (2003). *Generalized Estimating Equations*. London: Chapman and Hall/CRC.

**Helleday, T., Lo, J., van Gent, D. C. and Engelward, B. P.** (2007). DNA double-strand break repair: from mechanistic understanding to cancer treatment. *DNA Repair (Amst.)* **6**, 923-935.

**Hickson, I., Zhao, Y., Richardson, C. J., Green, S. J., Martin, N. M., Orr, A. I., Reaper, P. M., Jackson, S. P., Curtin, N. J. and Smith, G. C.** (2004). Identification and characterization of a novel and specific inhibitor of the ataxia-telangiectasia mutated kinase ATM. *Cancer Res.* **64**, 9152-9159.

**Huang, L. E., Bindra, R. S., Glazer, P. M. and Harris, A. L.** (2007). Hypoxia-induced genetic instability – a calculated mechanism underlying tumor progression. *J. Mol. Med.* **85**, 139-148.

**Jackman, R. P., Utter, G. H., Heitman, J. W., Hirschkorn, D. F., Law, J. P., Gefter, N., Busch, M. P. and Norris, P. J.** (2011). Effects of blood sample age at time of separation on measured cytokine concentrations in human plasma. *Clin. Vaccine Immunol.* **18**, 318-326.

**Jeggo, P. A. and Lobrich, M.** (2007). DNA double-strand breaks: their cellular and clinical impact? *Oncogene* **26**, 7717-7719.

**Kaspler, P., Pintilie, M. and Hill, R. P.** (2009). Dynamics of micronuclei in rat skin fibroblasts after X irradiation. *Radiat. Res.* **172**, 106-113.

**Lara, P. C., Lloret, M., Clavo, B., Apolinario, R. M., Bordon, E., Rey, A., Falcon, O., Alonso, A. R. and Belka, C.** (2008). Hypoxia downregulates Ku70/80 expression in cervical carcinoma tumors. *Radiother. Oncol.* **89**, 222-226.

**Lee, J. H., Choi, I. J., Song, D. K. and Kim, D. K.** (2010). Genetic instability in the human lymphocyte exposed to hypoxia. *Cancer Genet. Cytogenet.* **196**, 83-88.

**Liang, K. and Zeger, S. L.** (1986). Longitudinal data analysis using generalized linear models. *Biometrika* **73**, 13-22.

**Little, J. B. and Nagasawa, H.** (1985). Effect of confluent holding on potentially lethal damage repair, cell cycle progression, and chromosomal aberrations in human normal and ataxia-telangiectasia fibroblasts. *Radiat. Res.* **101**, 81-93.

**Little, J. B., Nagasawa, H., Dahlberg, W. K., Zdzienicka, M. Z., Burma, S. and Chen, D. J.** (2002). Differing responses of Nijmegen breakage syndrome and ataxia telangiectasia cells to ionizing radiation. *Radiat. Res.* **158**, 319-326.

**Liu, S. K., Coackley, C., Krause, M., Jalali, F., Chan, N. and Bristow, R. G.** (2008). A novel poly(ADP-ribose) polymerase inhibitor, ABT-888, radiosensitizes malignant human cell lines under hypoxia. *Radiother. Oncol.* **88**, 258-268.

**Marconi, V. C., Grandits, G., Okulicz, J. F., Wortmann, G., Ganesan, A., Crum-Cianflone, N., Polis, M., Landrum, M., Dolan, M. J., Ahuja, S. K. et al.** (2011). Cumulative viral load and virologic decay patterns after antiretroviral therapy in HIV-infected subjects influence CD4 recovery and AIDS. *PLoS ONE* **6**, e17956.

**Meng, A. X., Jalali, F., Cuddihy, A., Chan, N., Bindra, R. S., Glazer, P. M. and Bristow, R. G.** (2005). Hypoxia down-regulates DNA double strand break repair gene expression in prostate cancer cells. *Radiother. Oncol.* **76**, 168-176.

**O'Driscoll, M. and Jeggo, P. A.** (2006). The role of double-strand break repair – insights from human genetics. *Nat. Rev. Genet.* **7**, 45-54.

**Olive, P. L. and Banath, J. P.** (2004). Phosphorylation of histone H2AX as a measure of radiosensitivity. *Int. J. Radiat. Oncol. Biol. Phys.* **58**, 331-335.

**Ozeri-Galai, E., Schwartz, M., Rahat, A. and Kerem, B.** (2008). Interplay between ATM and ATR in the regulation of common fragile site stability. *Oncogene* **27**, 2109-2117.

**Paull, T. T., Rogakou, E. P., Yamazaki, V., Kirchgessner, C. U., Gellert, M. and Bonner, W. M.** (2000). A critical role for histone H2AX in recruitment of repair factors to nuclear foci after DNA damage. *Curr. Biol.* **10**, 886-895.

**Revai, K., Patel, J. A., Grady, J. J., Nair, S., Matalon, R. and Chonmaitree, T.** (2009). Association between cytokine gene polymorphisms and risk for upper respiratory tract infection and acute otitis media. *Clin. Infect. Dis.* **49**, 257-261.

**Rogakou, E. P., Pilch, D. R., Orr, A. H., Ivanova, V. S. and Bonner, W. M.** (1998). DNA double-stranded breaks induce histone H2AX phosphorylation on serine 139. *J. Biol. Chem.* **273**, 5858-5868.

**Sprong, D., Janssen, H. L., Vens, C. and Begg, A. C.** (2006). Resistance of hypoxic cells to ionizing radiation is influenced by homologous recombination status. *Int. J. Radiat. Oncol. Biol. Phys.* **64**, 562-572.

**Stiff, T., O'Driscoll, M., Rief, N., Iwabuchi, K., Lobrich, M. and Jeggo, P. A.** (2004). ATM and DNA-PK function redundantly to phosphorylate H2AX after exposure to ionizing radiation. *Cancer Res.* **64**, 2390-2396.

**Um, J. H., Kang, C. D., Bae, J. H., Shin, G. G., Kim, D. W., Kim, D. W., Chung, B. S. and Kim, S. H.** (2004). Association of DNA-dependent protein kinase with hypoxia inducible factor-1 and its implication in resistance to anticancer drugs in hypoxic tumor cells. *Exp. Mol. Med.* **36**, 233-242.

**Weichselbaum, R. R., Withers, H. R., Tomkinson, K. and Little, J.** (1983). Potentially lethal damage repair (PLDR) in X-irradiated cultures of a normal human diploid fibroblast cell strain. *Int. J. Radiat. Biol. Relat. Stud. Phys. Chem. Med.* **43**, 313-319.

**Wu, W., Wang, M., Wu, W., Singh, S. K., Mussfeldt, T. and Iliakis, G.** (2008). Repair of radiation induced DNA double strand breaks by backup NHEJ is enhanced in G2. *DNA Repair (Amst.)* **7**, 329-338.

Journal of Cell Science

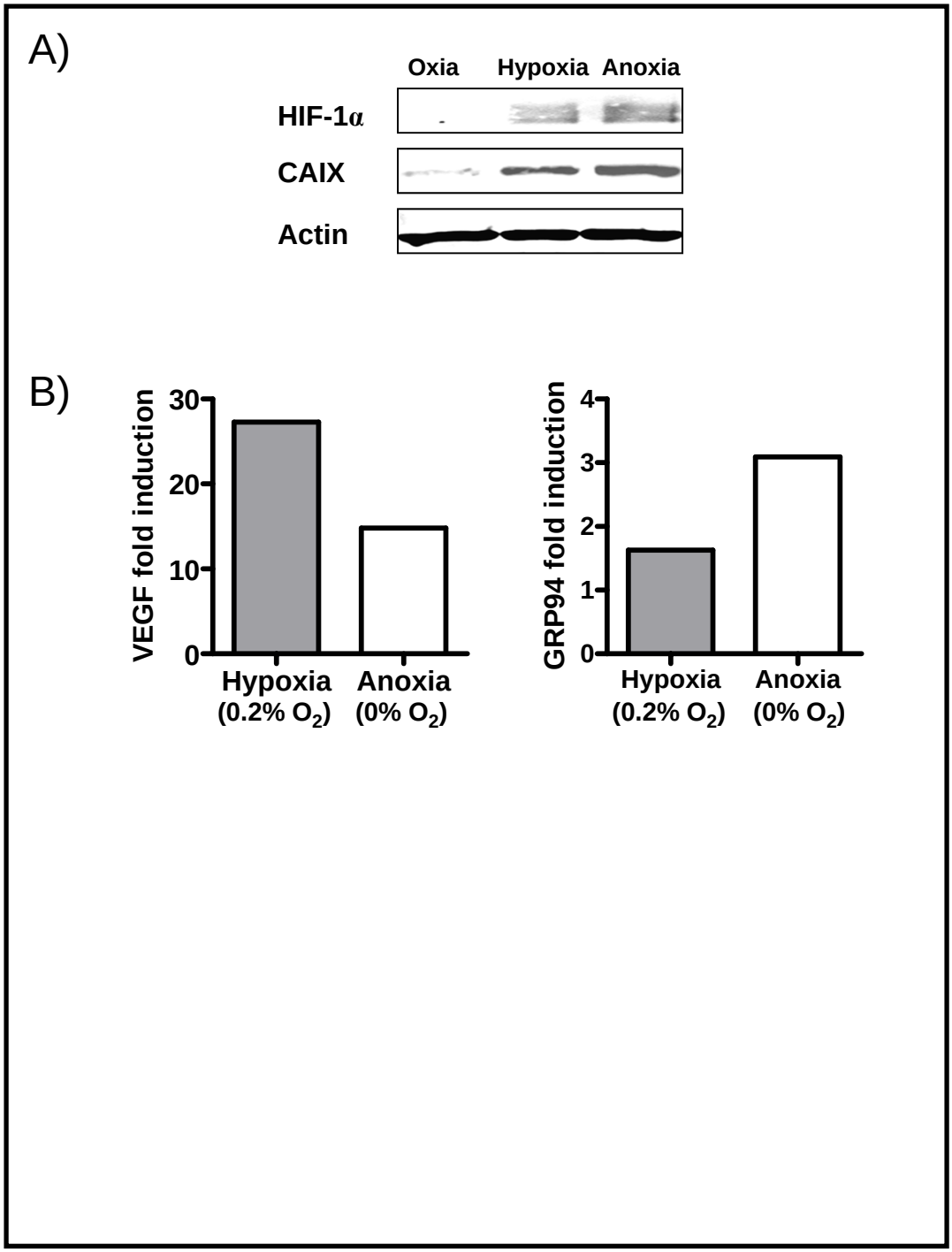
A)
Oxia
Hypoxia
Anoxia
HIF-1α
CAIX
Actin
B)
VEGF fold induction
30
20
10
0
Hypoxia (0.2% O2)
Anoxia (0% O2)
GRP94 fold induction
4
3
2
1
0
Hypoxia (0.2% O2)
Anoxia (0% O2)

*Figure S1*

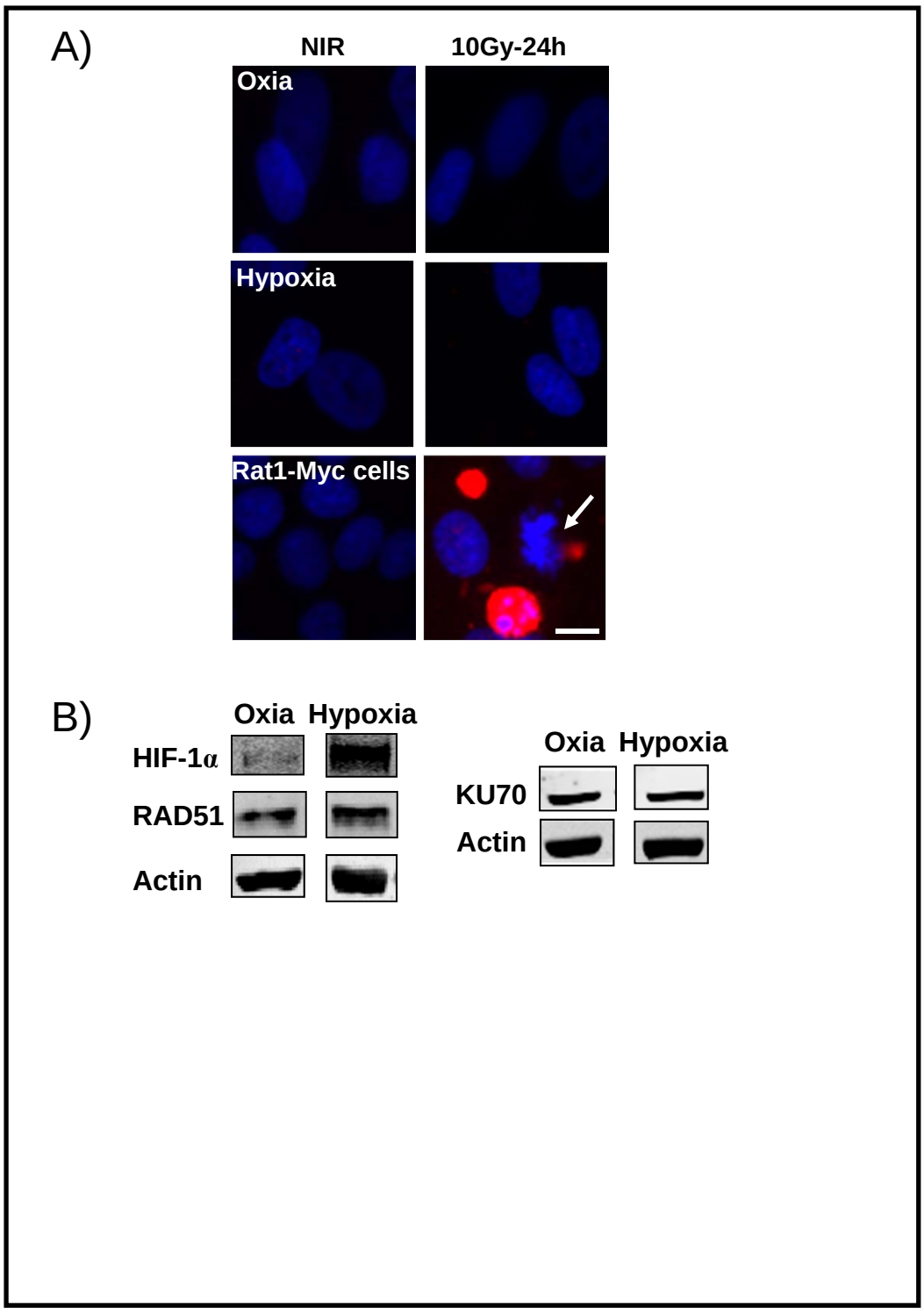
A)
NIR
10Gy-24h
Oxia
Hypoxia
Rat1-Myc cells
B)
Oxia
Hypoxia
HIF-1α
RAD51
Actin
Oxia
Hypoxia
KU70
Actin

*Figure S2*

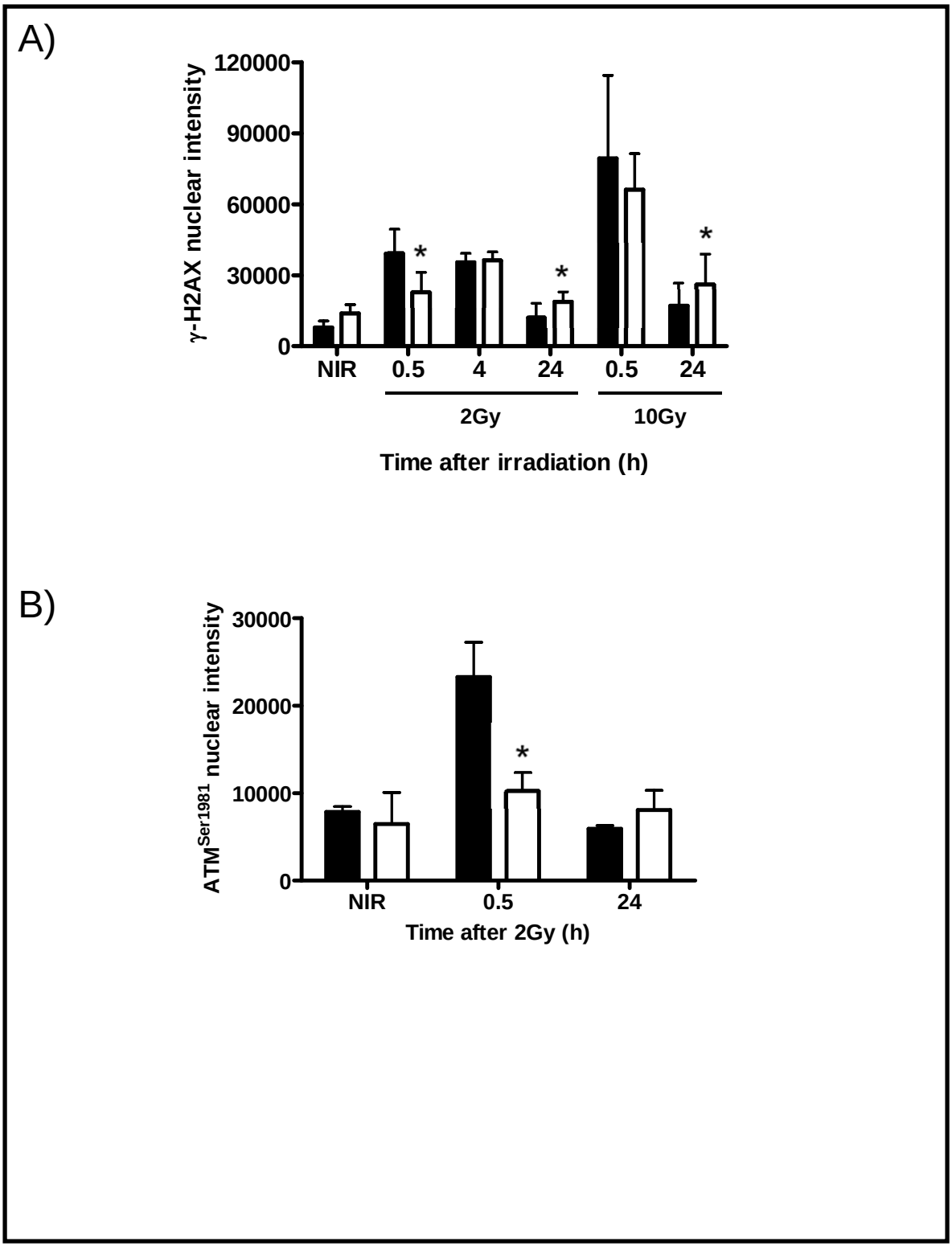
A)
120000
90000
60000
30000
0
γ-H2AX nuclear intensity
*
*
*
NIR
0.5
4
24
0.5
24
2Gy
10Gy
Time after irradiation (h)
B)
30000
20000
10000
0
ATM Ser1981 nuclear intensity
*
NIR
0.5
24
Time after 2Gy (h)

*Figure S3*

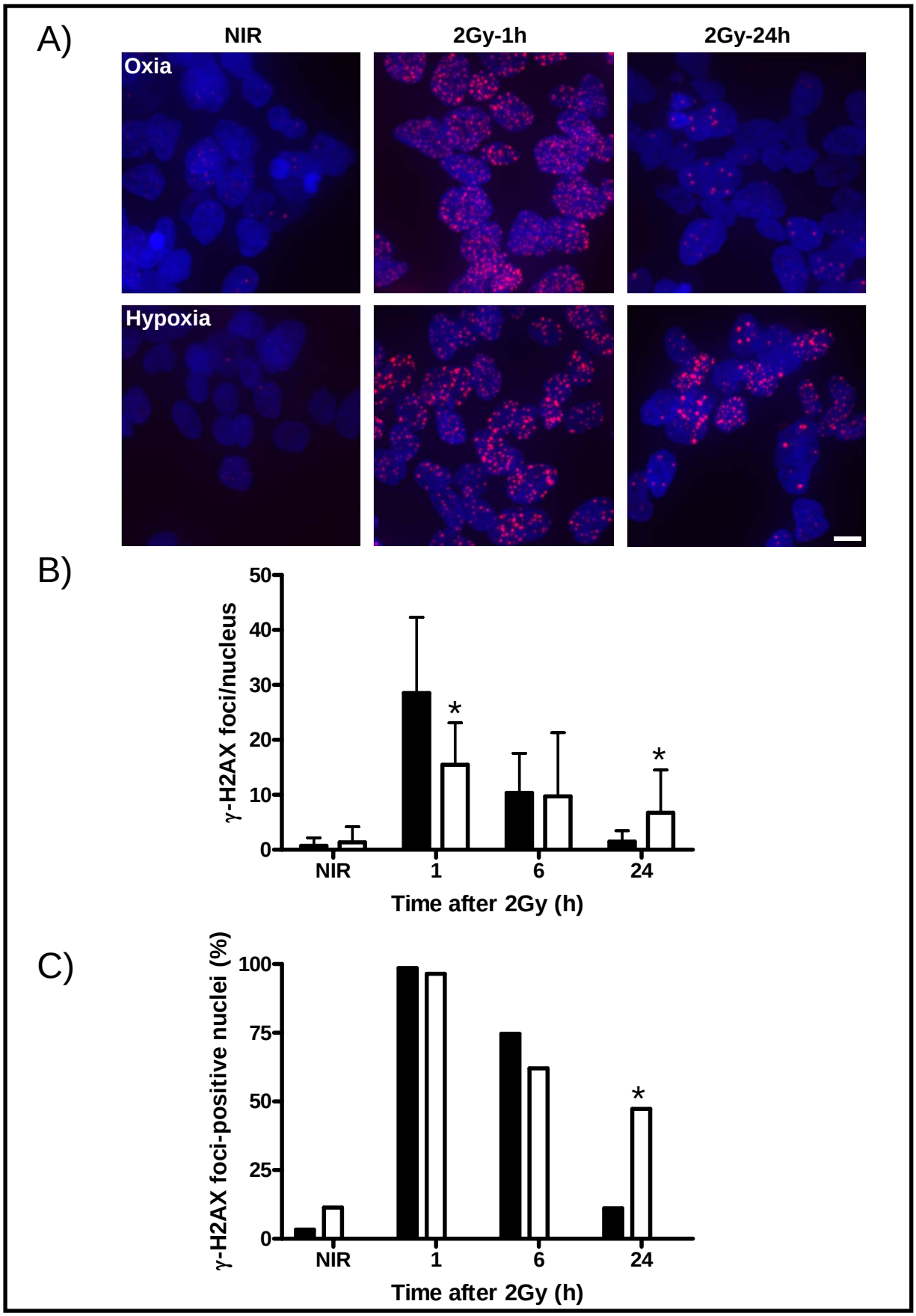
A)
NIR
2Gy-1h
2Gy-24h
Oxia
Hypoxia
B)
γ-H2AX foci/nucleus
50
40
30
20
10
0
*
*
NIR
1
6
24
Time after 2Gy (h)
C)
γ-H2AX foci-positive nuclei (%)
100
75
50
25
0
*
NIR
1
6
24
Time after 2Gy (h)

*Figure S4*

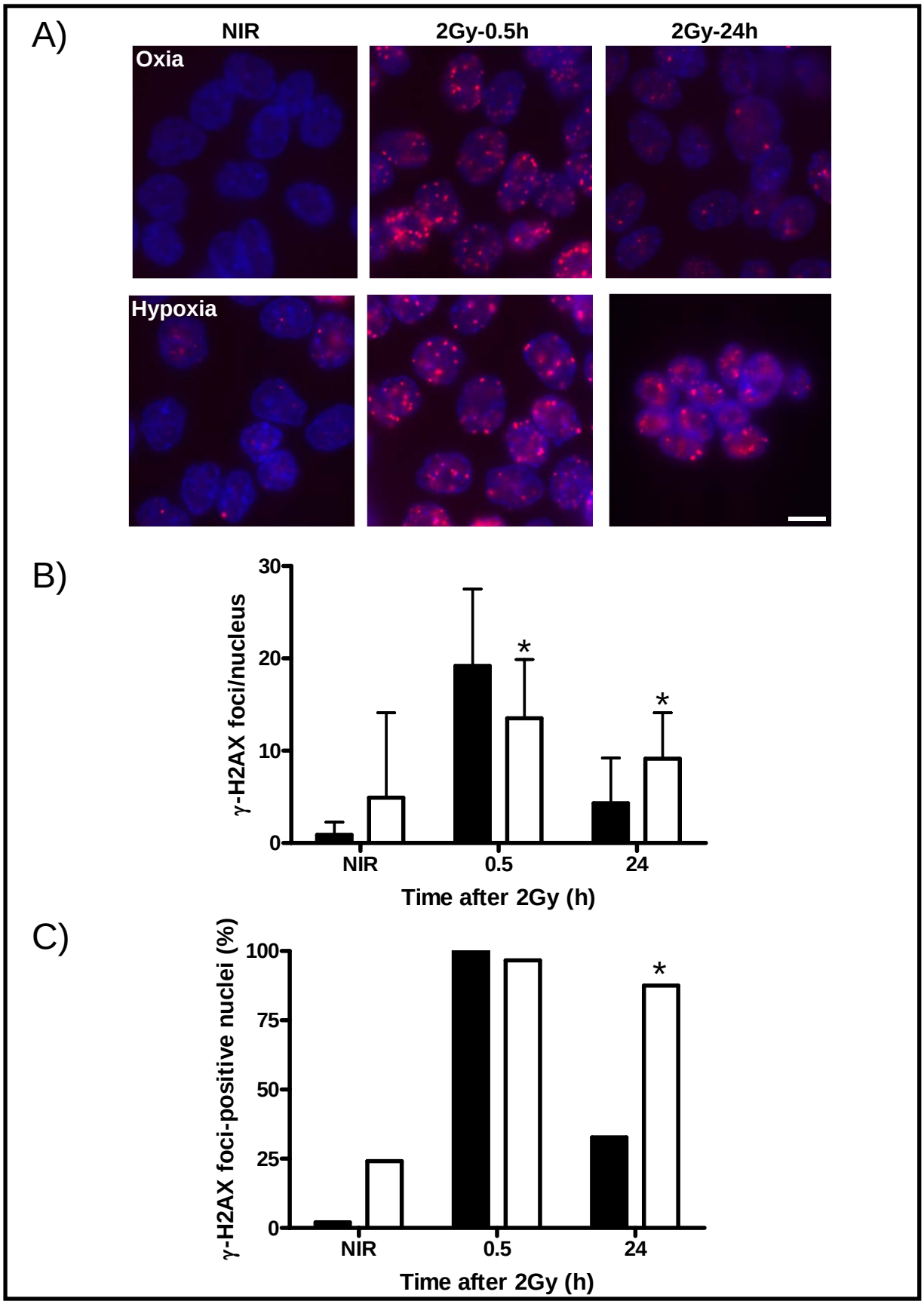
A)
NIR
2Gy-0.5h
2Gy-24h
Oxia
Hypoxia
B)
γ-H2AX foci/nucleus
30
20
10
0
*
*
NIR
0.5
24
Time after 2Gy (h)
C)
γ-H2AX foci-positive nuclei (%)
100
75
50
25
0
*
NIR
0.5
24
Time after 2Gy (h)

*Figure S5*

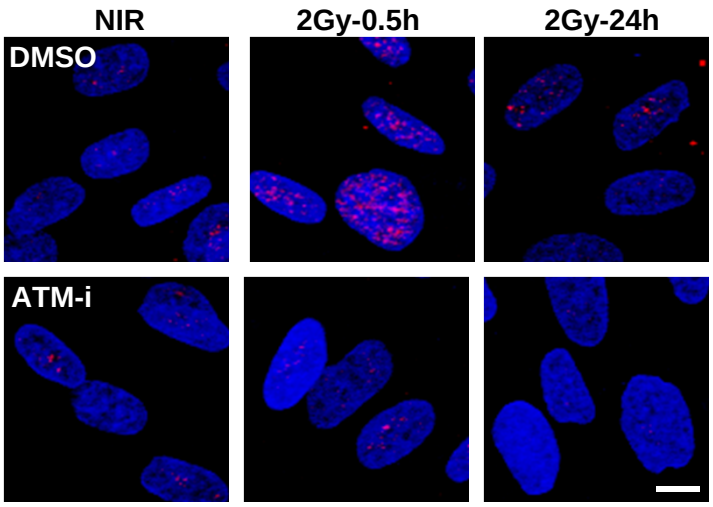


*Figure S6*

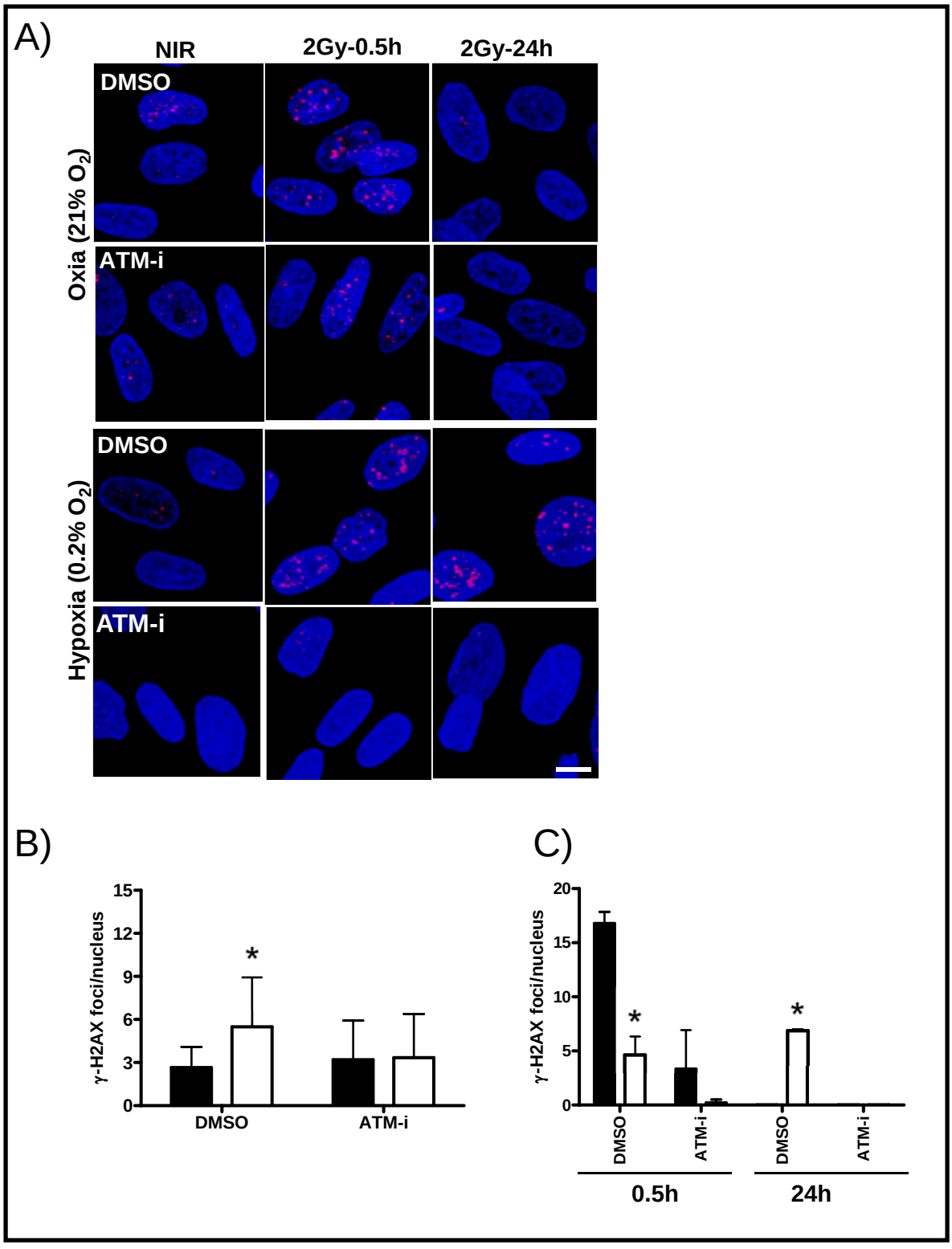
A)
NIR
2Gy-0.5h
2Gy-24h
DMSO
ATM-i
Oxia (21% O2)
DMSO
ATM-i
Hypoxia (0.2% O2)
B)
γ-H2AX foci/nucleus
15
12
9
6
3
0
*
DMSO
ATM-i
C)
γ-H2AX foci/nucleus
20
15
10
5
0
*
*
DMSO
ATM-i
DMSO
ATM-i
0.5h
24h

*Figure S7*

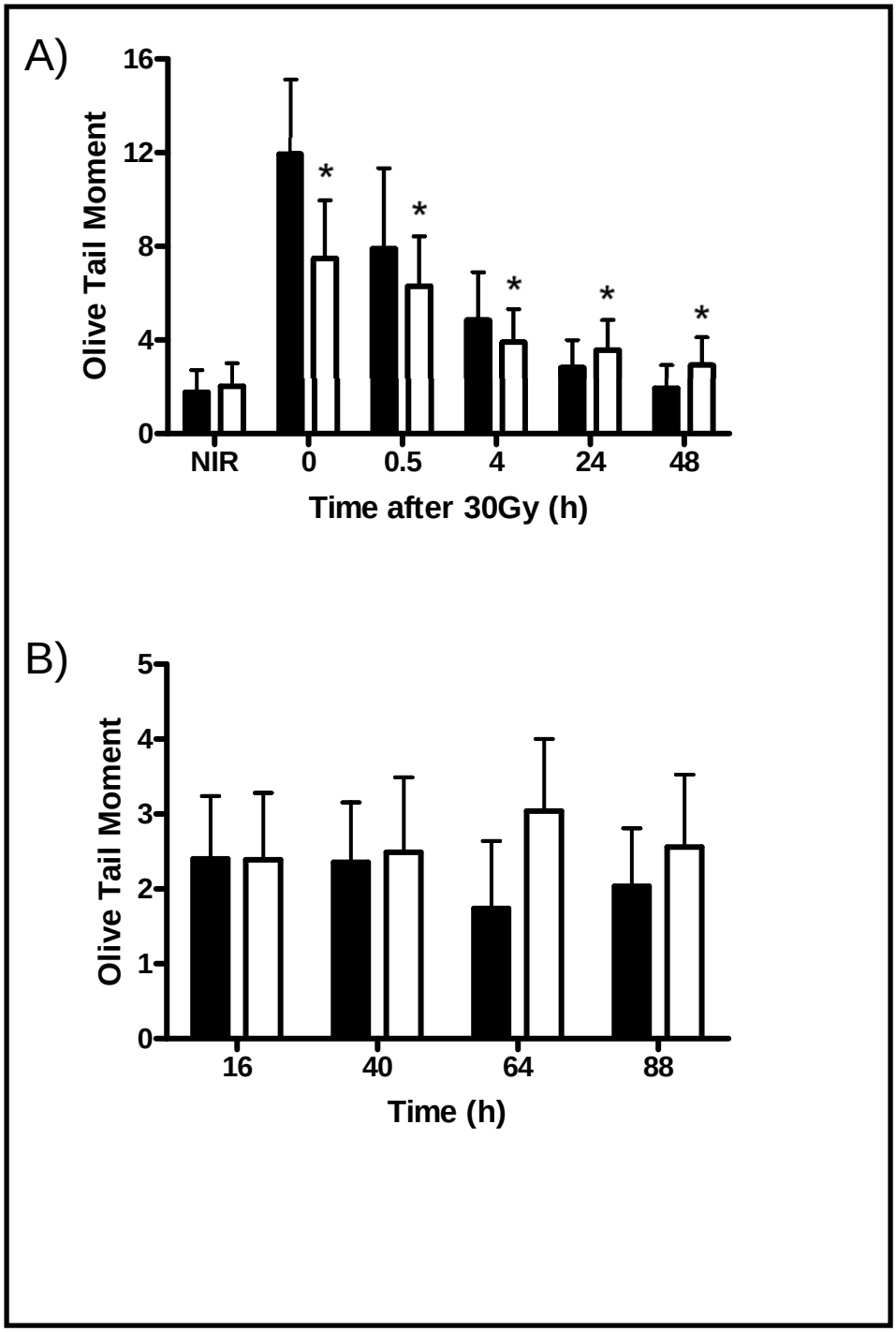
A)
Olive Tail Moment
16
12
8
4
0
*
*
*
*
*
NIR
0
0.5
4
24
48
Time after 30Gy (h)
B)
Olive Tail Moment
5
4
3
2
1
0
16
40
64
88
Time (h)

*Figure S8*

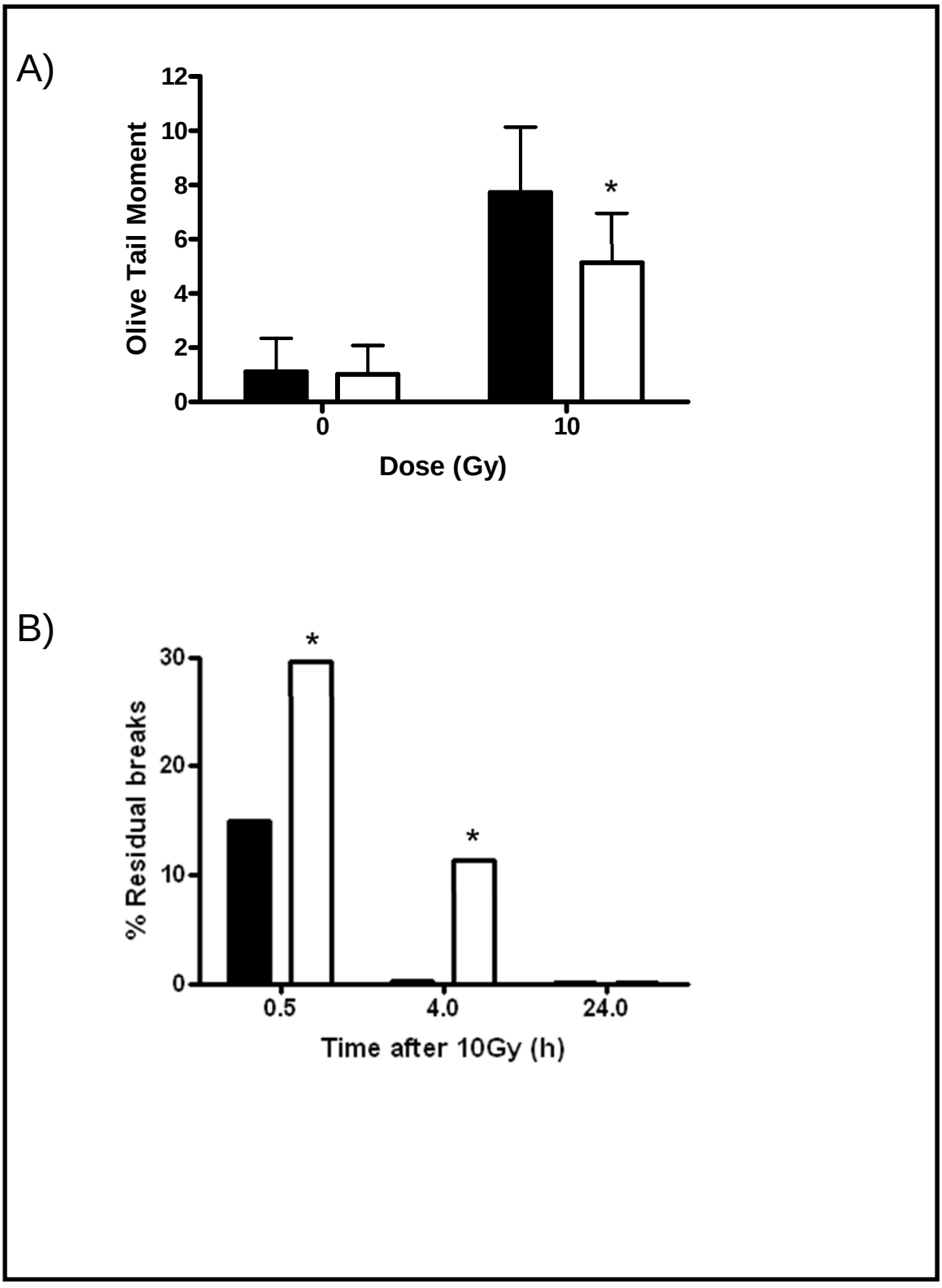
A)
Olive Tail Moment
12
10
8
6
4
2
0
*
0
10
Dose (Gy)
B)
% Residual breaks
30
20
10
0
*
*
0.5
4.0
24.0
Time after 10Gy (h)

*Figure S9*

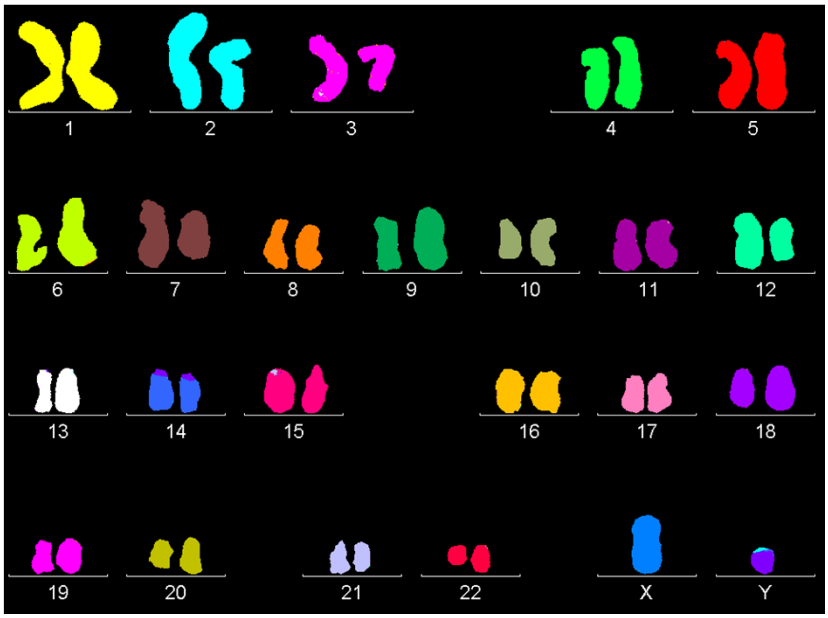


*Figure S10*